ADVANCED ENERGY MATERIALS
www.advenergymat.de

Toward Emerging Sodium-Based Energy Storage Technologies: From Performance to Sustainability

Zhen Xu and Jing Wang**

As one of the potential alternatives to current lithium-ion batteries, sodium-based energy storage technologies including sodium batteries and capacitors are widely attracting increasing attention from both industry and academia. However, the performance and sustainability of current sodium-based energy storage devices mostly rely on various critical materials and traditional energy-consuming fabrication processes. Meanwhile, the detailed working mechanisms of some sodium-based energy storage technologies are still under debate. Hence, how to realize low-cost, sustainable, and high-performance sodium-based energy storage technologies remains challenging from the perspective of theoretical studies, material diversification, and device optimization. In this review, the development state of sodium-based energy storage technologies from research background to principles is comprehensively discussed, as well as the advantages and disadvantages of state-of-the-art sodium-based energy storage devices are systematically analyzed, thus providing critical insight into the challenges and opportunities for emerging sodium-based energy storage technologies to achieve not only improved performance, but also enhanced sustainability.

1. Introduction

The lithium-ion battery technologies awarded by the Nobel Prize in Chemistry in 2019 have created a rechargeable world with greatly enhanced energy storage efficiency, thus facilitating various applications including portable electronics, electric vehicles, and grid energy storage.[1] Unfortunately, lithium-based energy storage technologies suffer from the limited resources (only 0.0017 wt% of lithium (Li) on Earth's crust) with a confined geographical availability (**Figure 1**), which is predicted to be insufficient for the global market in the near future.[2] Many strategies, hence, have been studied to relieve this emergency, including designing higher-energy lithiumless cells,[3] upcycling end-of-life devices,[4] and developing alternative technologies.[5] Among these solutions, the sodium-based energy storage technologies gradually become a promising successor to the current lithium-based technologies in the field of grid energy storage and low-speed electric vehicles due to the abundant resources of sodium (2.3 wt% of sodium (Na) on Earth's crust) and its similar properties to lithium, which has been listed as the key technology toward carbon neutrality in many countries.[6]

Based on varied working principles, sodium-based energy storage technologies can be further categorized into sodium batteries and capacitors to fulfill different energy and power requirements of the market. First, sodium-ion batteries represent the most typical device operating based on the classic "rocking-chair" principle where sodium ions move from the cathode side to the anode side during the charging process.[7] The state-of-the-art sodium-ion batteries possess an energy density of around 200 Wh kg^{-1} close to the commercial lithium-ion batteries based on the $LiFePO_4$ cathode (**Figure 2**).[8] Aiming to obtain higher power, sodium-ion capacitors are fabricated through the dual-ion mechanism where the sodium ions insert into the anode, whilst the counter ions are adsorbed on the cathode during the charging process.[9] With the combination of the capacitor-type cathode and the battery-type anode, sodium-ion capacitors can realize an energy density between 10 and 200 Wh kg^{-1} with a power density from 10 000 to 100 W kg^{-1} (Figure 2).[10] Furthermore, sodium metal batteries are established to pursue higher energy with the metallic sodium anode whose theoretical capacity is 1166 mAh g^{-1}.[11] Differing from the typical anodes in sodium-ion batteries, the metallic sodium anode stores cations based on the redox pairs of Na^+/Na instead of the insertion or conversion mechanism.[12] By coupling with high-energy cathodes such as sulfur cathode or oxygen cathode, the energy density is estimated to reach over 350 Wh kg^{-1} or even close to 500 Wh kg^{-1} (Figure 2).[13] In general, the development of sodium-ion batteries has the potential to enter the industrial production stage,[14] while the

Z. Xu
Yusuf Hamied Department of Chemistry
University of Cambridge
Cambridge CB2 1EW, UK
E-mail: zx293@cam.ac.uk
J. Wang
Bristol Composites Institute (ACCIS)
School of Civil
Aerospace, and Mechanical Engineering
University of Bristol
Bristol BS8 1TR, UK
E-mail: jw17476@bristol.ac.uk

The ORCID identification number(s) for the author(s) of this article can be found under https://doi.org/10.1002/aenm.202201692.

DOI: 10.1002/aenm.202201692

Figure 1. The distribution of lithium resources around the world. Reproduced with permission.[6] Copyright 2021, Springer Nature.

demonstration of sodium-ion capacitors and sodium metal batteries remains at the lab-scale level,[10,12] which both need more effort from scientists and engineers to overcome their corresponding significant challenges such as the lack of low-cost, high-performance, and sustainable electrode materials as well as cost-effective electrolyte systems for the final commercialization of these technologies. Hence, the engineering optimization of sodium-ion batteries and the scientific innovation of sodium-ion capacitors and sodium metal batteries are becoming one of the most important research directions in the community of energy storage currently.

During the development of sodium-based energy storage technologies, the sustainability of electrode materials and electrolytes is an easily overlooked factor for the whole system, thus questioning the overall sustainability of sodium-based energy storage technologies. As we know, the performance and the cost of energy storage devices were the most concerning factors in the industry. Nevertheless, with the gradual emergence of environmental issues in traditional manufacturing industries, the sustainability of energy storage devices is also arousing the attention of the whole community. For example, hard carbons consisting of short-range graphitic domains and long-range amorphous features have been widely applied as not only conductive agents and active materials but also functional hosts on account of their low cost, high electronic conductivity and stable physicochemical properties.[16] However, most hard carbons are derived from nonrenewable fossil fuels using high-temperature carbonization or chemical activation process.[17] At the same time, the structural features of hard carbons containing morphologies, surface chemistries, defects, and pores are complicated to be accurately tuned by those conventional carbonization methods.[16] Therefore, advanced material design strategies are needed to address those issues of electrode materials including hard carbons and thus enhance the overall sustainability of sodium-based energy storage technologies.

In this review, the relative working principles of sodium-based energy storage are summarized, along with a comparison to lithium-based technologies. Afterward, the recent research progress of specific sodium-based energy storage technologies is reviewed including the whole technological platform from material synthesis to cell configuration, and the corresponding challenges remaining to be addressed are critically analyzed. Meanwhile, a perspective on the necessity and promises of sustainable materials for addressing the existing issues of sodium-based energy storage technologies is also discussed, based on the current situations of utilizing materials in those technologies. This review aims to benefit the rational design of sodium-based energy storage technologies with not only improved performance but also enhanced sustainability.

2. Sodium-Based Energy Storage Technologies

As we know, harvested clean energy needs a suitable place to store, and sodium-based energy storage technologies including sodium batteries and capacitors become the most promising choices because of their low cost, enhanced sustainability, and appropriate capacity now.[6] However, when we look into the history of sodium-based energy storage technologies, the development of sodium batteries and capacitors was not plain sailing although it happened side-by-side with the lithium batteries since the 1970s.[18] At the very beginning, metallic anodes were employed in the prototype cells,

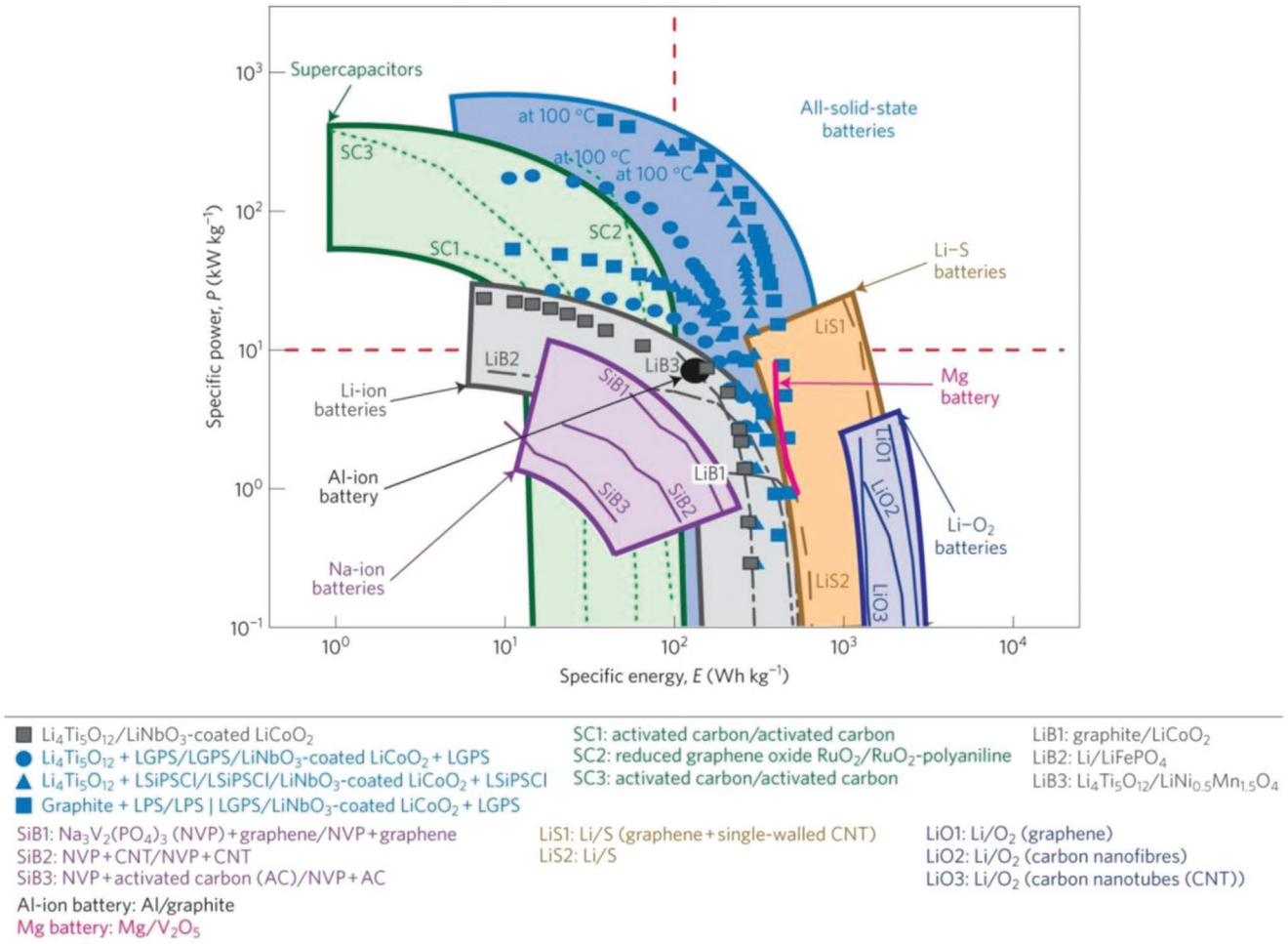

Figure 2. The Ragone plot of different types of energy storage devices. Reproduced with permission.[15] Copyright 2016, Springer Nature.

but the high risk of short circuits due to the metallic dendrite formation questioned the commercialization of lithium and sodium batteries.[19] When scientists discovered that readily available graphite can be a perfect host material for lithium ions rather than sodium ions, the promise of commercializing lithium-ion batteries finally exceeded that of sodium batteries in the 1990s,[20] thus underestimating the value of sodium-based energy storage technologies for a long time. Nevertheless, with the successful commercialization and growing demands of lithium-ion batteries in the worldwide market (**Figure 3**a), the shortage and uneven distribution of lithium recourse gradually attract global attention.[21] Driven by this situation, sodium-based energy storage technologies witnessed a revival in concern since the 2010s (Figure 3b).

Based on these research backgrounds, the basic knowledge and fundamental understanding of sodium batteries and capacitors are first introduced and compared with lithium-based energy storage in the following sections. After that, the recent progress of sodium batteries and capacitors is also summarized to critically analyze the state-of-the-art challenges and research directions in these fields, thus clearly stating the research background, significance, and development approaches of low-cost, sustainable, and high-performance sodium-based energy storage technologies.

2.1. Definitions, Principles, and Metrics

2.1.1. Definitions and Principles

For sodium batteries and capacitors, the working principles highly depend on the type of electrode materials. First of all, sodium-ion batteries are the most typical type of sodium batteries based on the "rocking-chair" mechanism, in which host materials of sodium ions are used as the electrodes (**Figure 4**a).[7] During the charging process, sodium ions move from the cathode to the anode through the electrolyte, while electrons move along the external circuit in the same direction. Meanwhile, the cathode materials are oxidized mostly through the deintercalation mechanism, while the anode materials are reduced according to three main mechanisms including insertion, conversion or alloying.[8] Since the whole progress is reversible, sodium-ion batteries belong to the rechargeable secondary batteries.

Furthermore, sodium metal batteries and their derivatives can be fabricated when using metallic sodium as the anode material. Based on the redox pairs of Na^+/Na, sodium metal anode can provide a low potential of −2.714 V versus standard hydrogen electrode (SHE) and an outstanding theoretical specific capacity of 1166 mAh g^{-1}.[12] When coupling with cathode

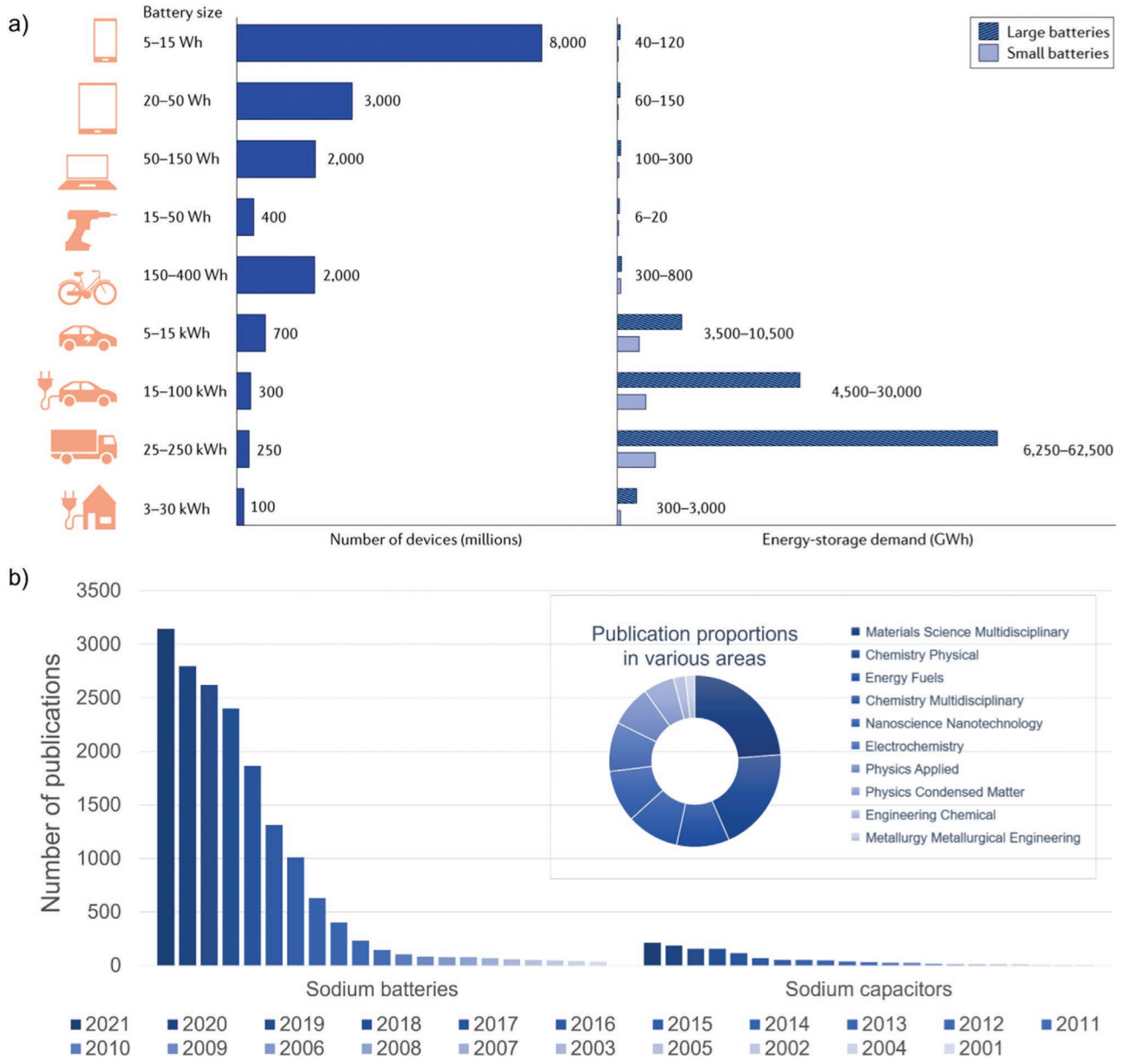

Figure 3. a) Estimated energy storage demand for 2016–2050. Reproduced with permission.[21] Copyright 2018, Springer Nature. b) Numbers of publications containing sodium batteries and capacitors since 2001 indexed by Web of Science with the inset of top ten related areas.

materials such as sulfur or oxygen according to different reaction mechanisms, the so-called sodium–sulfur or sodium–oxygen batteries can be achieved with ultrahigh energy densities.[12] All these technologies using sodium metal anodes can be collectively referred to as sodium metal batteries. In short, sodium batteries are mainly composed of sodium-ion batteries and sodium metal batteries at the time of writing.

Apart from sodium batteries employing the single-ion strategy, sodium capacitors apply the dual-ion mechanism where sodium ions across the electric double layer and enter the bulk phase of the anode materials, while counter ions are mainly adsorbed on the surface of the cathode materials during the charging process (Figure 4b).[10] Namely, the Faradic redox reactions happen inside the anode, and the non-Faradic physical accumulation of ions dominates at the cathode side.[22] Without using sodium metal anodes, sodium capacitors can be called sodium-ion hybrid capacitors in normal circumstances. Combined with the battery-type anode and the capacitor-type cathode, sodium capacitors have the potential to bridge the gap between sodium batteries and supercapacitors, possessing excellent power and energy simultaneously.[9] The brief categories of sodium-based energy storage technologies are shown in Figure 4c.

2.1.2. Metrics

The systems of measuring the electrochemical performance of sodium batteries and capacitors are similar, containing specific

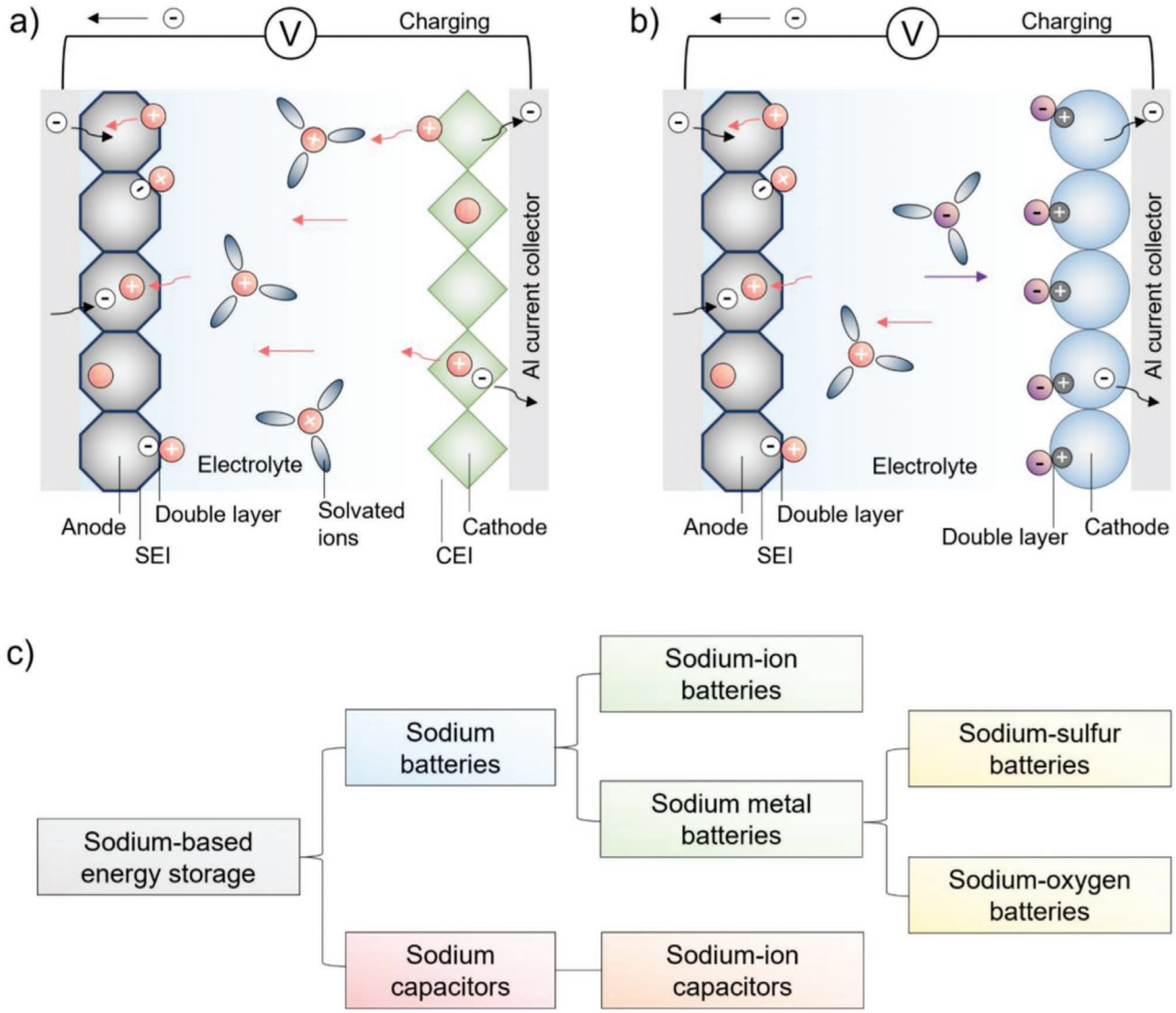

Figure 4. The schematic illustrations of working principles of a) sodium batteries, and b) sodium capacitors. c) The brief categories of sodium-based energy storage technologies.

capacity, energy and power densities, rate and cycling performance, and Coulombic efficiency. Sodium capacitors can also be evaluated based on the specific capacitance. In addition, sustainability is currently becoming an important evaluation metric for sodium batteries and capacitors.

For experimental results, the charge or discharge specific capacitance and capacity of the working electrodes in half cell configurations can be calculated from galvanostatic charge–discharge (GCD) curves (**Figure 5**) according to Equations (1) and (2), respectively[16]

$$C_{\text{electrode}} = \frac{I\Delta t}{m\Delta U} \tag{1}$$

$$Q_{\text{electrode}} = \frac{I\Delta t}{3.6m} \tag{2}$$

where $C_{\text{electrode}}$ (F g^{-1}) refers to the discharge or charge specific capacitance of the working electrodes, while $Q_{\text{electrode}}$ (mAh g^{-1}) is the discharge or charge specific capacity. I (A) is the constant discharge or charge current. ΔU ($=U_{\max}-IR_{\text{drop}}-U_{\min}$, V) is the working voltage window, and m (g) is the mass of active material loaded on the working electrodes. Δt (s) is the discharge or charge time. Notably, Equation (1) is only suitable for nearly linear GCD curves such as GCD curves based on capacitor-type reactions (Figure 5b). For batteries, the plateau regions of GCD curves correspond to the redox peaks in cyclic voltammetry (CV) curves (Figure 5a). For hybrid capacitors, the GCD curves of typical full cells are a combination of the GCD curves of their anode and cathode, and so are their CV curves (Figure 5c). The power and energy densities of the full cells can be calculated using Equations (3) and (4)[16]

$$E_{\text{device}} = \frac{I}{3.6M}\int_{t_1}^{t_2} U(t)\,\mathrm{d}t \tag{3}$$

$$P_{device} = \frac{3600E_{device}}{\Delta t} \quad (4)$$

where E_{device} (Wh kg^{-1}) and P_{device} (W kg^{-1}) are the energy and power densities of devices, respectively. I (A), M (g), and Δt (s) are the constant discharge or charge current, the total mass of active materials in both anodes and cathodes, and the discharge or charge time, respectively. In addition, $U(t)$ is the voltage that changes with time under galvanostatic discharging or charging, t_1 is the start time of charge/discharge processes, and t_2 is the end time. Therefore, increases in the discharge or charge time, and working voltage windows with a decreased amount of active mass can enhance the energy density of the device under a constant current. Simultaneously, the power density will increase. Importantly, the other inactive components of devices including the encapsulation materials, current collectors, electrolytes, and binders should be stable under such a working voltage window. When it comes to the industry level, the M for calculating the energy density will include not only the mass of active materials but also the total weight of the whole device containing those inactive components.

In theoretical situations, the specific capacity of materials as an electrode can be calculated based on the converted Faraday's law of equation (5)[23]

$$Q_t = \frac{nF}{3.6m} \quad (5)$$

where Q_t, n, F, and m are the theoretical capacity, the number of transferred electrons, the Faraday constant (96 485 C mol^{-1}), and the molecular mass of the active material. Furthermore, the energy density can also be theoretically determined according to the Nernst formula of Equation (6)[24]

$$\Delta_r G = \Delta_f G_p - \Delta_f G_r \quad (6)$$

where $\Delta_r G$, $\Delta_f G_p$, and $\Delta_f G_r$ are the Gibbs free energy of a chemical reaction, the formulation energy of the reactants, and the formulation energy of the products, respectively. Afterward, $\Delta_r G$ can be converted into the maximum electrical work of this chemical reaction as shown in Equation (7)[24]

$$\Delta_r G = -nFE \quad (7)$$

where n and E are the number of transferred electrons of one-mole reactant and the thermodynamic equilibrium voltage, respectively, because $\Delta_f G_p - \Delta_f G_r$ is equal to $-nFE$. Meanwhile, the theoretical energy density is defined as[24]

$$\varepsilon_M = \frac{\Delta_r G}{\sum M} \quad (8)$$

where ε_M and $\sum M$ are the theoretical energy density and the sum of mole mass of all the reactants, respectively. With the combination of Equations (7) and (8), the theoretical energy density can be finally calculated as follows

$$\varepsilon_M = \frac{-nFE}{\sum M} \quad (9)$$

Therefore, to increase the energy density in theoretical situations, we need to look for an electrochemical reaction that can transfer a higher concentration of electrons. Also, the

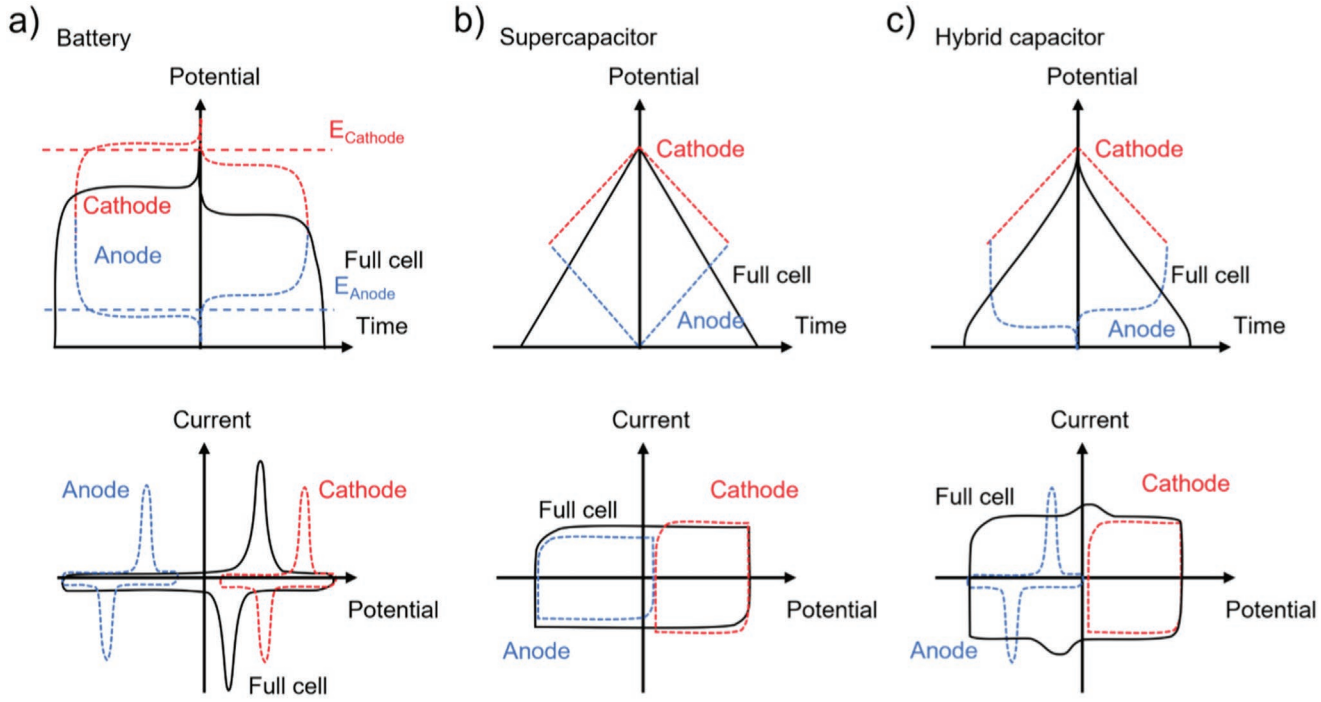

Figure 5. The typical GCD curves of the cathode, anode and full cell and their corresponding CV curves in a) battery, b) supercapacitor, and c) hybrid capacitor.

larger differences in the equilibrium potentials between the products and reactants are, the higher energy density can be obtained.

Rate and cycling performance are another two key parameters to evaluate the electrochemical performance of devices, which represents their fast charge–discharge capabilities and lifetime.[25] These two metrics can be tested using the galvanostatic charge–discharge process under different current densities with different cycle numbers. For the rate performance, the polarization phenomena of the cell, including the concentration polarization, electrochemical polarization, and ohmic polarization, can induce unfavorable decreases in the cell voltage and specific capacities at a higher current density (**Figure 6**a).[26] First of all, the concentration polarization means the existence of ionic concentration gradients in the electrolyte, which is related to the ion transfer kinetics in the electrolyte.[27] For example, with a fast depletion of ions at the electrode boundary, the slower ion transfer kinetic in the electrolyte can cause a larger concentration polarization. In addition, the electrochemical polarization is related to the kinetics of ion transfer at the electrode–electrolyte interface and inside the electrode.[26] For instance, when the applied electronic currents in the external circuit increase, the faster kinetics of ion transfer at the electrode–electrolyte interface and inside the electrode, along with a faster electrochemical reaction, can lead to less electrochemical polarization. Meanwhile, the lower intrinsic electrical resistance of the cell components can result in the weaker ohmic polarization during the fast charge–discharge process.[27] Unlike mass transport-derived concentration polarization, the corresponding response time of ion transfer in the liquid electrolyte should be quicker than the ion transfer at the electrode–electrolyte interface and inside the electrode.[28] Besides, the reaction-driven response time should be the slowest among them, while the electron migration is the fastest. For the cycling performance, the stability of the electrode, electrolyte, and their interface as well as the reversibility of electrochemical reactions are all highly involved in the lifetime of devices. In brief, the physicochemical properties of each component in the device affect the rate and cycling performance.

The Coulombic efficiency in each cycle also matters because the Coulombic efficiency describes the reversibility and stability of electrochemical reactions, which is highly linked with the cycling performance.[29] The Coulombic efficiency of anodes in the half cell configuration is equal to the ratio of the charge capacity to the discharge capacity, while in the half cells of cathodes or full cells, the Coulombic efficiency is equal to the ratio of the discharge capacity to the charge capacity. The irreversible capacity in each cycle results from the so-called "dead" sodium, including sodium for the solid electrolyte interphase (SEI) formation, sodium trapped in electrode structures and isolated sodium after cycling.[30] First, since SEI mainly forms in the first cycle, the initial Coulombic efficiency (ICE) can be defined to evaluate the SEI formation. In principle, if the lowest unoccupied molecular orbital (LUMO) of electrolytes is lower than the Fermi level (μA) of anodes, the electrons will transfer from μA of the anode to LUMO of electrolytes when currents are applied, indicating the reduction of electrolytes in the first cycle (Figure 6b).[31] Also, if the highest occupied molecular orbital (HOMO) of electrolytes is higher than the Fermi level (μ_C) of cathodes, the electrons will transfer from HOMO of electrolytes to μ_C of cathodes, which means the oxidation of electrolytes.[31] Afterward, a passivation SEI layer will be formed from the decomposition of electrolytes to fully cover electrodes as a barrier to prevent the direct electron transfer with electrolytes.[32] A higher ICE means fewer sodium ions needed for producing excessive SEI, which can save active materials. If the interface

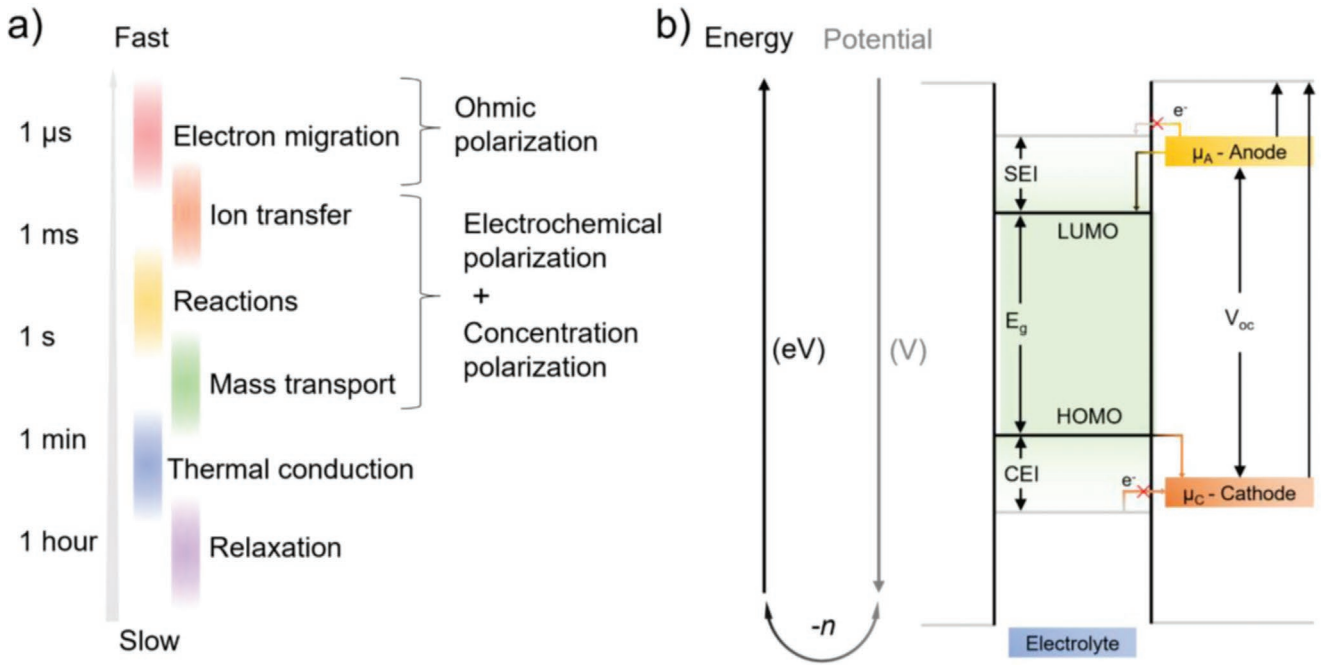

Figure 6. a) Dynamics of polarization in typical energy storage devices. b) The schematic diagram of the energy levels and potentials of electrodes and electrolytes with the formation of solid electrolyte interphase (SEI) and CEI (i.e., the SEI at the cathode side).

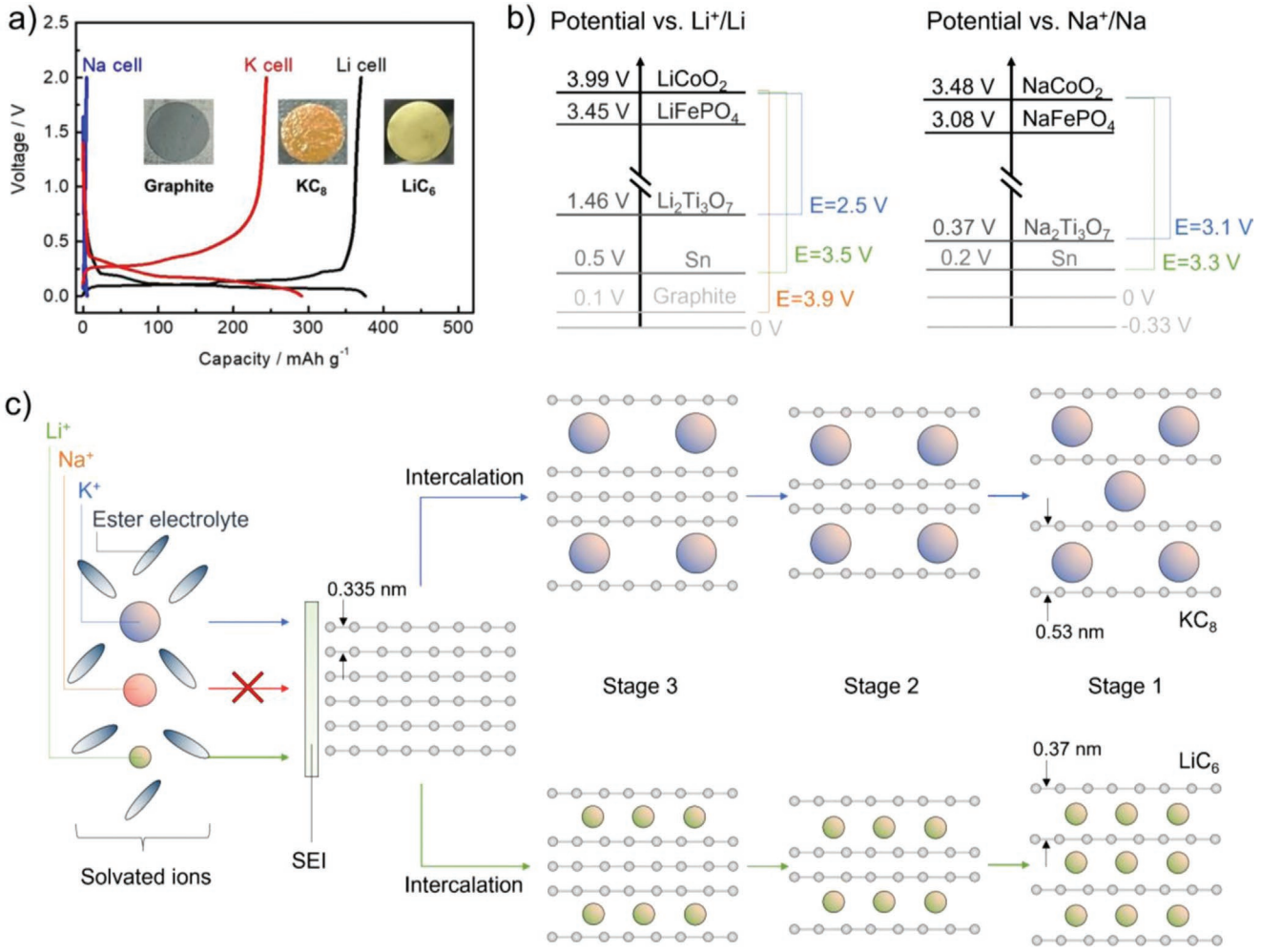

Figure 7. a) The typical discharge–charge curves of graphite anodes to store cations in the half cell configuration with the inset photography of graphite and graphite intercalation compounds including LiC_6 and KC_8. Reproduced with permission.[42] Copyright 2018, Wiley. b) The redox potentials of electrode materials versus Li^+/Li or Na^+/Na (data source collected from ref. [41]). c) The schematic illustrations of intercalation behaviors of lithium and potassium ions into graphite in ester electrolytes.

is unstable, SEI layers will break and reform over and over again during cycling with a low Coulombic efficiency in each cycle.[33] Therefore, stabilizing SEI at the interface is of great importance for cycling performance. Except for SEI formation, sodium trapped in the electrode structures can also decrease the Coulombic efficiency, which is related to the inherent reversibility of sodium storage reactions and the accessibility of ion pathways within the electrode structure.[34] Last but not least, the isolated sodium due to the pulverization of electrodes during cycling can reduce the Coulombic efficiency as well.[35] Generally, the optimization of electrolytes and electrodes can contribute to the improvement of the Coulombic efficiency in each cycle. An ICE of over 80% and the Coulombic efficiency of ≈99.9% after the first cycle are desirable for devices with an ideal reversibility and cycling performance.[36]

For evaluating the sustainability of materials and devices, life cycle assessment can be a key and powerful tool to deliver the environmental information.[37] Through the theoretical calculation from the life cycle perspective, the CO_2 emissions of each stage within the fabrication of sodium-based energy storage devices from material preparation to cell assembly can be estimated, which can provide a reference for the comparison to current commercial lithium-ion batteries.[38] Except for CO_2 emissions, the life cycle assessment can tell the possibility of land acidification, water pollution and many other environmental issues during the whole fabrication process. Also, based on the difference in raw material and power suppliers, the life cycle assessment can exhibit the environmental effects of the fabrication process on different countries and areas. With the improvement of the evaluation system of sustainability, we believe that the life cycle assessment will play an increasingly important role in the field of energy storage.

2.1.3. Comparisons to Lithium

Both as alkali metals, sodium and lithium are located in the first main group on the periodic table, which indicates that they are similar but not exactly the same. For example, the ionic radius and molar mass of sodium are inherently larger than those

of lithium.[39] Compared to lithium, the natural properties of sodium lead to the detailed discrepancies in its electrochemical behaviors, and thus mainly obstruct the previous development of sodium-based energy storage technologies. On one hand, sodium ions can rarely intercalate into graphite which is a cost-effective anode material to store lithium ions (**Figure 7**a).[40] On the other hand, since the redox potential of sodium is higher than that of lithium, the energy of sodium-based full cells with the narrower working voltage window is theocratically lower than that of lithium-based ones in most cases (Figure 7b).[41]

As mentioned above, the successful application of graphite anodes has greatly contributed to the initial industrialization of lithium-ion batteries. Until now, graphite still dominates the choice of anode materials, although the lithium cathode materials have achieved tremendous progress from $LiCoO_2$ to $LiFePO_4$ and $LiNi_{0.8}Mn_{0.1}Co_{0.1}O_2$.[43] At the very beginning, scientists assume that the too large size of sodium ions fails their intercalation into graphite. However, this explanation actually oversimplified the truth because potassium ions with an even larger ionic radius of 1.38 Å than sodium ions can still allow the intercalation into graphite (Figure 7c).[44] The graphite intercalation compounds (GICs) formed by lithium and potassium ions are LiC_6 and KC_8, respectively, and thus the theoretical capacities of graphite to store lithium and potassium ions are 372 and 279 mAh g^{-1}, correspondingly (Figure 7a).[45] By contrast, the GIC formation of NaC_{64} is predicted with a low theoretical capacity of 35 mAh g^{-1}, which implies sodium ions can hardly intercalate into the graphite lattices.[46] Therefore, rare intercalation of sodium ions into graphite does not result from the large size of sodium ions. According to van der Waals density functional theory calculations, the formation enthalpies of NaC_6 or NaC_8 are positive, so the formation of sodium-rich GICs needs a redox potential below 0 V versus Na^+/Na,[46] where the precipitation of sodium metal will take place first forever. When the redox potential is positive, the interaction between sodium ions and in-plane graphene layers is too weak to stabilize the formed GICs.[47] Moreover, the stokes radius and desolvation energy of sodium ions in traditional ester electrolytes are even smaller than those of lithium ions (**Table 1**). Hence, the intercalation of lithium ions into graphite is, in fact, the abnormal existence with a negative formation enthalpy of LiC_6.[47] To overcome these intrinsic shortcomings of sodium ions, great efforts have been made by scientists to develop efficient and durable sodium-ion storage materials.

However, because of the abundant resources (**Figure 8**a) as well as smaller stokes radius and desolvation energy of sodium ions (Table 1),[48] sodium-based energy storage devices still have a number of advantages such as low cost and better possible electrochemical performance under higher operation currents or lower running temperatures in comparison to current lithium-based ones (Figure 8b).[49] In addition, there is one more potential advantage of sodium-based energy storage devices for their energy density, which is the possible usage of lighter and cheaper aluminum current collectors on both sides (Figure 8a).[49] In commercial lithium-ion batteries, the anode can only employ copper foils as the current collector as lithium alloys with aluminum under a specific potential. The usage of aluminum current collectors, however, can greatly contribute to the increased energy density, decreased fabrication cost, and enhanced sustainability of sodium-based energy storage devices (Figure 8b). To sum up, how to replace critical materials in current battery technologies with abundant and renewable materials is a significant research direction to achieve the balance between performance and sustainability of sodium-based energy storage devices (Figure 8c). Detailed examples will be provided in the following case study parts.

Table 1. Comparison of sodium and lithium's properties (Reproduced with permissions.[6,7] Copyright 2021, Springer Nature and Copyright 2014, American Chemical Society).

Element	Ionic radius [Å]	Molar mass [g mol^{-1}]	Redox potential [V vs SHE]	Stokes radius in PC[a)] [Å]	Desolvation energy in PC [kJ mol^{-1}]
Sodium	1.02	23.0	−2.71	4.6	157.3
Lithium	0.76	6.9	−3.04	4.8	218.0

[a)] PC: propylene carbonate.

2.2. Sodium Batteries

According to the visualized statistics of keywords in publications related to sodium batteries (**Figure 9**), it is the performance of sodium batteries that attracts the greatest attention from scientists. Compared to cathodes and electrolytes, anodes are mentioned more regularly in recent literature, which indicates the importance of anodes for the current stage of sodium batteries. Meanwhile, anode materials like graphene, reduced graphene oxide, carbon nanotube, carbon nanofiber, hard carbon, MoS_2, and anatase TiO_2 are frequently reported. Therefore, carbon materials for sodium-ion batteries become the most popular research direction, along with the latest average publication year and the strong links with other keywords. In addition, P2-type layered metal oxide, $Na_3V_2(PO_4)_3$, and Prussian blue dominate the choices of cathode materials. It is worth noting that most publications care about the performance and cost of sodium batteries, but the sustainability hardly exists in Figure 9, further indicating that the sustainability of sodium batteries has been seriously ignored.

As discussed above, the physicochemical properties of electrodes and electrolytes occupy a significant position in determining the electrochemical performance and sustainability of sodium batteries, hereby the detailed case studies and corresponding critical analysis are provided to deepen the understanding of the specific correlations.

2.2.1. Anodes

The mentioned anode materials for sodium batteries can be correspondingly categorized according to their different kinds of mechanisms including insertion, alloying, and conversion.[52] In addition, metallic sodium can be employed as the anode directly to achieve a high energy density based on the redox couple of Na^+/Na.[53]

Insertion-Type: This type of anode material as the host material for sodium ions usually possesses high electrochemical stability and reversibility. Graphite has been the benchmark anode material to store lithium ions in the industry since the

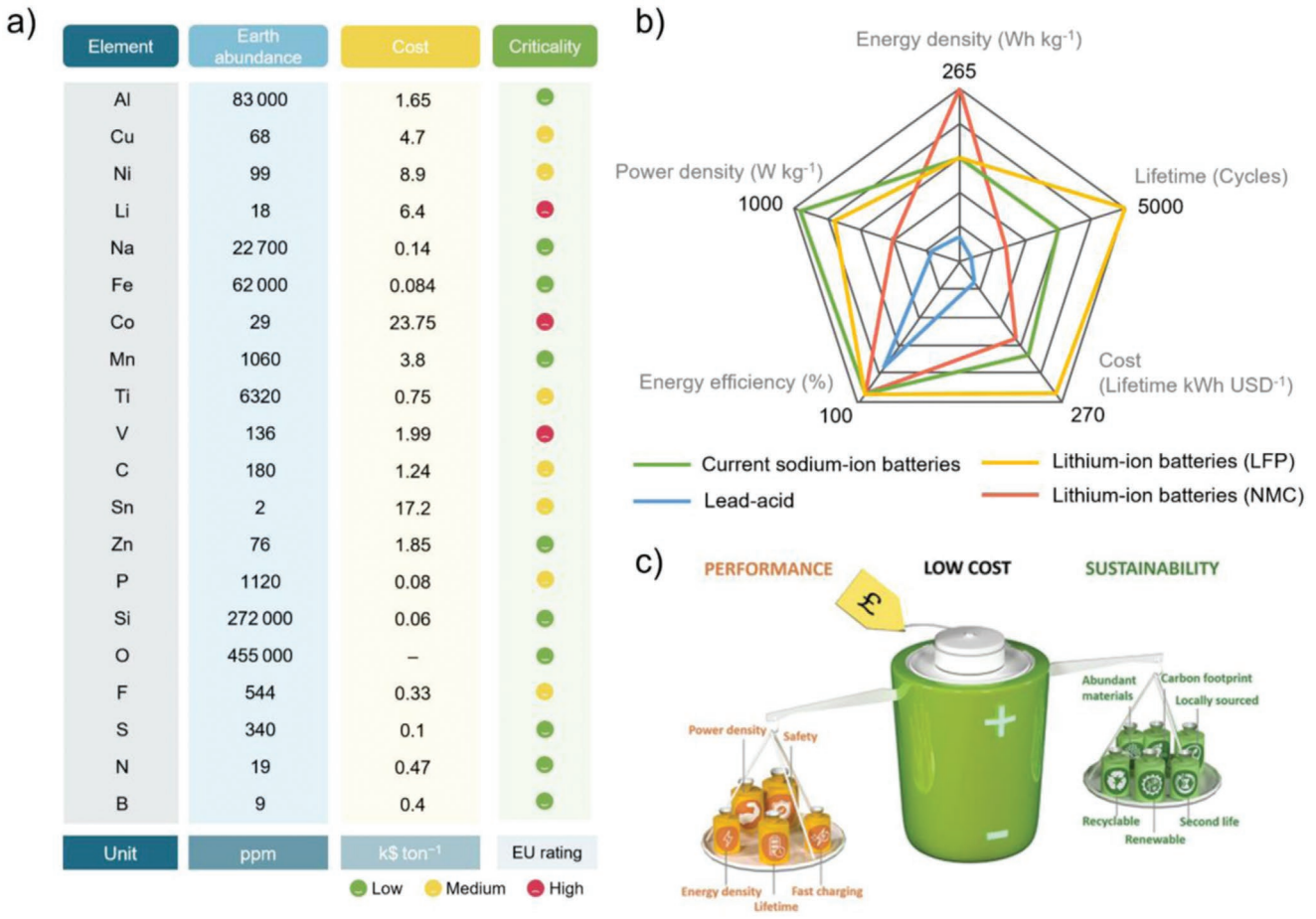

Figure 8. a) Earth abundance, cost, and criticality of elements in battery technologies (data source collected from ref. [48]). b) The radar plot of the comparison between current lead-acid, lithium-ion, and sodium-ion batteries regarding the power density, energy density, energy efficiency, lifetime, and cost (data source collected from ref. [50]). c) The schematic illustration of the balance between performance and sustainability of sodium-based energy storage technologies. Reproduced with permission.[51] Copyright 2021, Wiley.

1990s, but unfortunately, the intercalation of sodium ions into graphite cannot happen without a solvent.[41] Sodium ions can only enter the graphite through the cointercalation together with ether-based electrolyte molecules, which can achieve a capacity of around 90 mAh g^{-1}.[41] Unlike graphite, amorphous carbons such as hard or soft carbons are discovered to be the suitable insertion-type candidate to store sodium ions with a reversible capacity of 250 to 300 mAh g^{-1}.[47] However, the detailed sodium-ion storage mechanism of amorphous carbons is still under debate, thus obstructing the rational design of high-performance carbon anodes.[47] Typically, amorphous carbons are composed of curved graphene layers, which are turbostratically stacked (**Figure 10**a). For the main differences between soft and hard carbons, soft carbons can still be graphitized at a high temperature like 2000 °C, but hard carbons cannot make it, which means hard carbons are generally more disordered than soft carbons in similar preparation circumstances (Figure 10a).[54] While various carbonaceous precursors including crosslinked polymers, coal and pitch can be utilized to synthesize amorphous carbons, the fossil fuel-based resources hinder the overall sustainability of sodium-ion batteries.[54] Hence, the bioinspired hard carbons represent a more sustainable choice of anode materials (Figure 10b). Until now, hard carbon anodes with capacities as high as 350–400 mAh g^{-1} have been reported with optimized pore and defect structures (Figure 10c).[55] Meanwhile, three derivative models have been established to explain the insertion mechanism of sodium ions in the sloping region and the plateau region of GCD curves, including "insertion–adsorption," "adsorption–insertion," and "adsorption–filling" models (Figure 10d–f).[56] In these models, "insertion" obviously represents the insertion of sodium ions into graphene layers of hard carbons, while "adsorption" and "filling" mean the adsorption of sodium ions onto defect sites of graphene layers and the sodium-ion filling into nanovoids, respectively.[56]

For example, Tang et al.[58] studied the structural effects on the electrochemical performance of glucose-derived hard carbons at 1000 °C. The reversible charge capacity of their hard anodes reached 168 mAh g^{-1} at 0.2 A g^{-1}. Even at 5 A g^{-1}, the charge capacity still reached 75 mAh g^{-1} since the obtained hollow carbon spheres with high porosity can shorten the ion diffusion pathway to active sites (**Figure 11**a). However, excessive opening pores also possess disadvantages. Li et al.[57] prepared a kind of cellulose-derived hard carbon anodes to store sodium ions. By

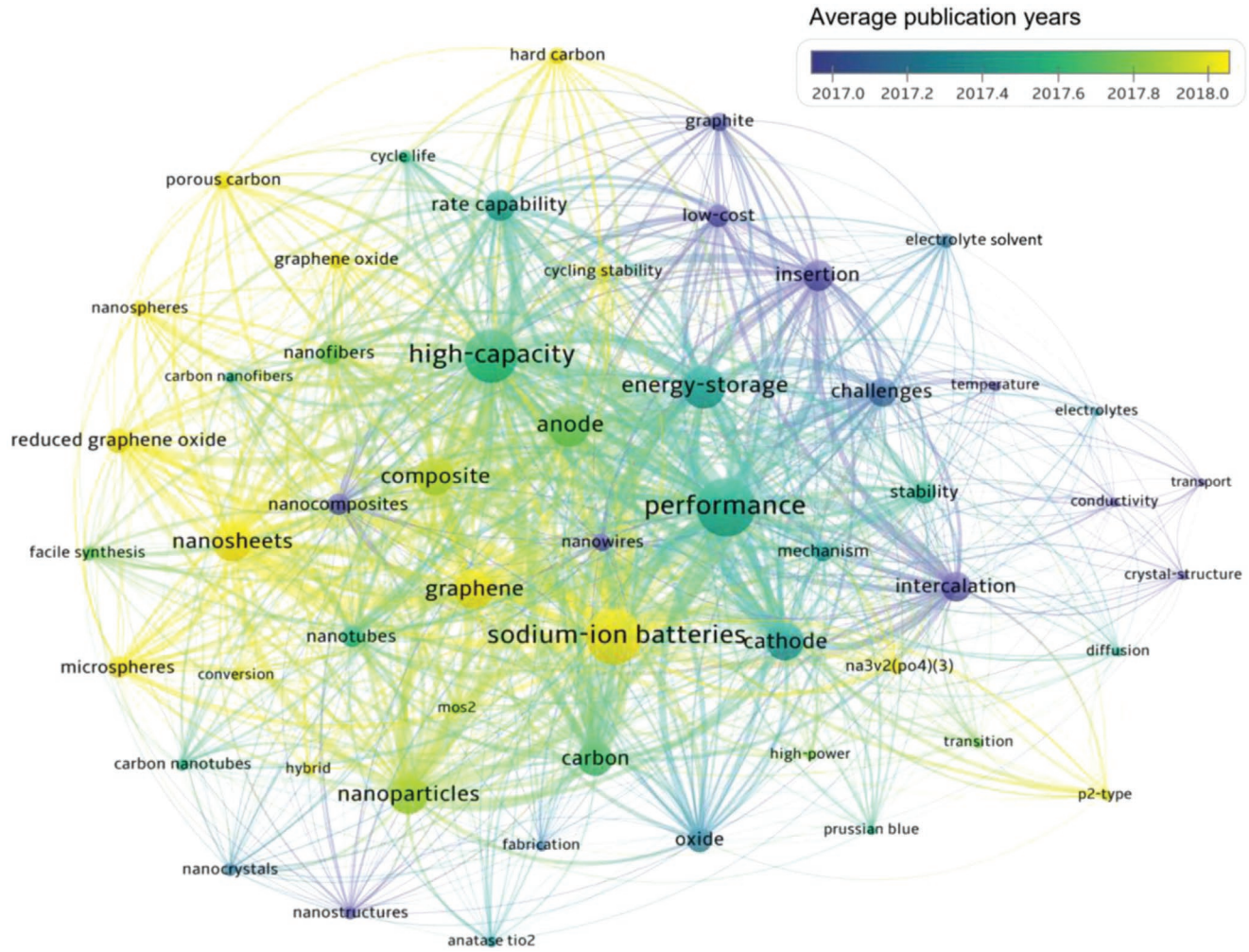

Figure 9. The visualized statistics of keywords in publications related to sodium batteries since 2001 indexed by Web of Science, where the color represents the average publication year, and the size indicates the reported frequency in the literature.

controlling the carbonization temperatures between 1000 and 1600 °C, the pore and defect structures of hard carbons can be tuned to achieve the optimized electrochemical performance. With the increase in temperatures, the decrease in accessible surface areas of hard carbons can be attributed to the closure of opening pores (Figure 11b). Under the carbonization temperature of 1300 °C, the highest reversible capacity of 315 mAh g^{-1} at 0.03 A g^{-1} was achieved in the half cell configuration of hard carbon electrodes with a suitable ICE of over 80%. By contrast, the hard carbon anodes prepared at 1000 °C only delivered the reversible capacity of around 100 mAh g^{-1} with a low ICE of 26%. The irreversible capacity mainly resulted from the excessive SEI formed on their huge accessible surface, so the modification of pore structures is essential to suppress unnecessary SEI formation. Except for pores, defects are also notable. Xu et al.[59] synthesized cellulose-derived hard carbon anodes with nitrogen and sulfur codoping for sodium-ion batteries. The obtained hard carbon showed a reversible charge capacity of 280 mAh g^{-1} at 0.03 A g^{-1} and an excellent rate retention of 46% at 10 A g^{-1}. In conjunction with theoretical calculations, they implied that the heteroatom-doping can produce more defects into hard carbons with enlarged interlayer spaces to reduce the diffusion barriers and provide more favorable sodium-ion interactions with defect sites (Figure 11c). To sum up, tuning the morphologies, pore and defect structures of bio-derived hard carbons can contribute to the improved electrochemical performance and enhanced sustainability of sodium-ion storage.

Furthermore, according to the correlations between hard carbon structures and electrochemical performance, Au et al.[60] claimed sodium ions were adsorbed on the defect sites in the sloping region, while the filling of sodium ions into closed nanovoids happened in the plateau region. This "adsorption–filling" mechanism model has also been confirmed by Stratford et al.[61] using advanced characterization methods like the pair distribution function analysis and operando solid-state ^{23}Na nuclear magnetic resonance (NMR). Interestingly, we can see from many reported studies that the shapes of GCD curves mostly depend on the interaction behaviors of sodium ions with active sites. For instance, the slope-dominated GCD curves represent the high-power features of hard carbons, which is related to the rapid kinetics of adsorbing sodium ions at defect sites (Figure 11d).[62] That is to say that the adsorption of sodium ions

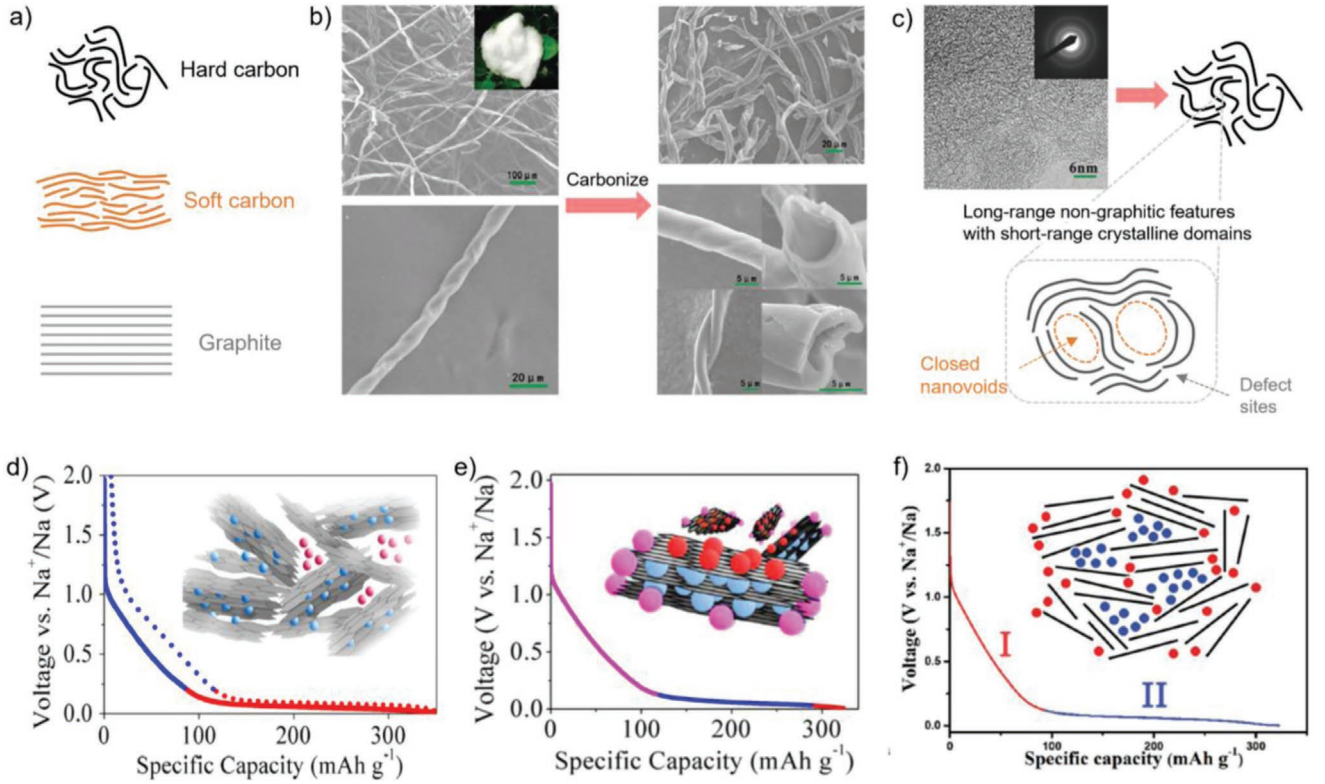

Figure 10. a) Schematic illustrations of inner structures of hard carbon, soft carbon, and graphite. b) Scanning electron microscopy (SEM) images of cellulose-rich cotton before and after the carbonization with the inset photography of cotton. Reproduced with permission.[57] Copyright 2016, Wiley. c) The transmission electron microscopy image of typical hard carbons with the illustrated active sites including closed nanovoids and defect sites. Reproduced with permission.[57] Copyright 2016, Wiley. The sodium-ion storage mechanism models of hard carbons including d) "insertion–adsorption", e) "adsorption–insertion", and f) "adsorption–filling" models. Reproduced with permission.[56] Copyright 2019, American Chemical Society.

at defect sites with a rapid kinetic can be considered as a kind of surface-controlled reaction. In contrast, the plateau-dominated GCD curves represent the high-energy features of hard carbons, linked with the sluggish kinetics of sodium-ion filling within closed nanopores (Figure 11e).[63] Namely, the filling of sodium ions within closed nanovoids with a slow kinetic can be considered as a kind of diffusion-controlled reaction. Since sodium ions will penetrate the solid electrolyte interphase and across the interface to combine with electrons, the sodium-ion storage behaviors demonstrated above both belong to the Faradic process.[64] Until now, the specific sodium-ion mechanisms in hard carbon are still uncertain, such as what the state of sodium stored inside the closed nanovoids is, and how sodium ions interact with different kinds of defect sites. Therefore, solid evidence is needed to prove these unknown details in hard carbons, thus paving the way for rationally preparing high-performance, low-cost, and sustainable hard carbons from biomass in the future.

As alternatives to hard carbons, some titanate, organic-based electrodes also provide reasonable capacities according to the insertion mechanism. For titanates such as TiO_2, $Li_4Ti_5O_{12}$, $Na_2Ti_3O_7$, $NaTiO_2$, and $NaTi_2(PO_4)_3$ based on different space groups (**Figure 12**a), they usually accommodate sodium ions through the reduction of Ti^{4+} into Ti^{3+} during the sodiation process (Figure 12b).[6] Their corresponding capacities can reach around 110 to 180 mAh g^{-1} as the critical elements contained in titanates are heavier than carbon.[66] Meanwhile, their redox potentials of around 1.0 versus Na^+/Na are higher than the plateau region of hard carbons (0.1 V vs Na^+/Na), which can present the dendrite formation but also decrease the energy density of the full cell.[66] The summaries and comparisons of redox potentials and capacities of different titanate-based anode materials are shown in Figure 12c.[65] In addition, the specific channel structures inside titanates can provide an outstanding rate and cycling performance with short ion diffusion pathways and small volume changes during the charge–discharge process.[67] In comparison to hard carbon anodes, the low electronic conductivity, expensive costs, and high redox potentials of titanates are challenging their future applications in battery industries.[68]

Given the low redox potentials and existence of active sites, some organics can also be used as solid-state anode materials to store sodium ions. In principals, functional groups like carboxylate, imine, and azo have redox activity at the low redox potentials.[69] For example, electrons of π bonds between oxygen and carbon atoms in carboxylate can be delocalized to oxygen and carbon atoms, and the polarized state of moieties can interact with sodium ions (**Figure 13**a).[69] During the sodiation process, the oxygen atom obtains one more electron from the initial state to bond with sodium atoms. The more redox-active sites in organic molecules can increase the storage ability of sodium ions, so the molecular engineering of organics to enhance the

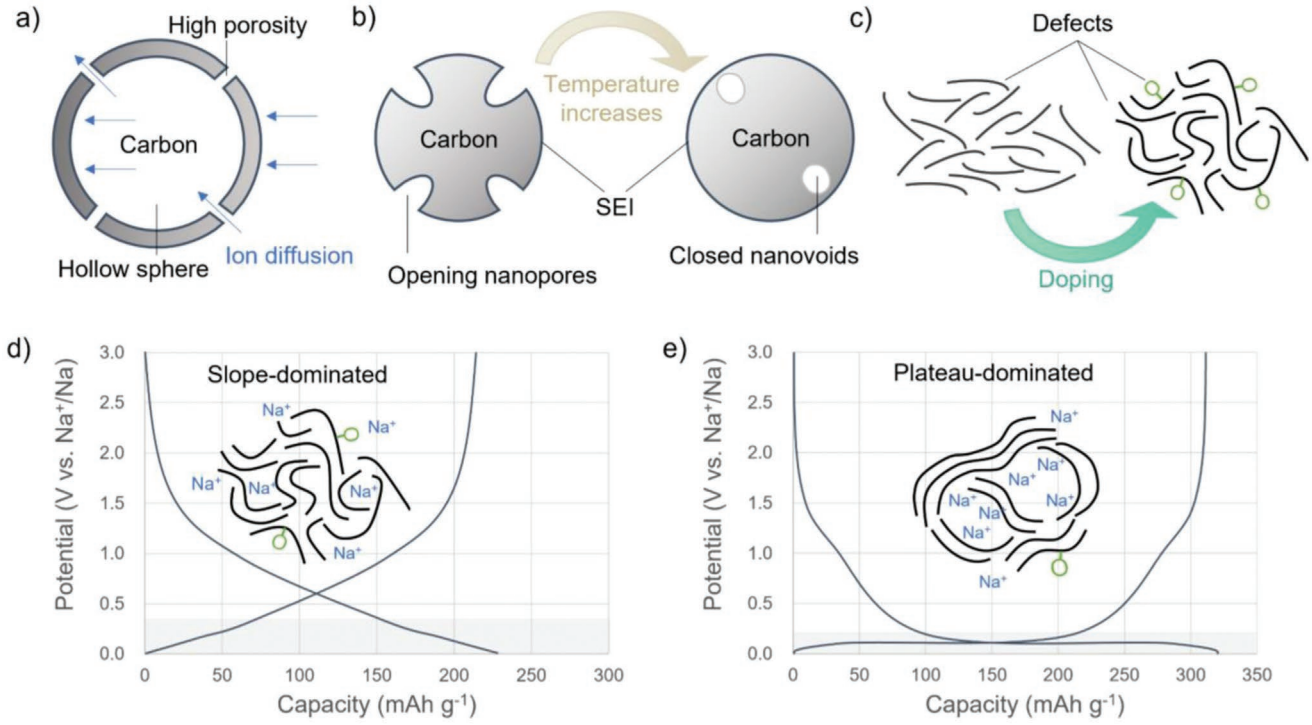

Figure 11. The modification of a) morphologies, b) pore, and c) defect structures of bio-derived hard carbons to enhance their electrochemical performance. d) The typical GCD curves of hard carbons dominated by the adsorption of sodium ions at defect sites. e) The typical GCD curves of hard carbons dominated by the filling of sodium ions within closed nanovoids.

active-site concentration is essential. The structures of some reported organic anode materials with their redox potentials are listed here (Figure 13b,d).[69] Among them, disodium terephthalate (Na_2TP) and its derivates are the most classical organics as the anode materials because of the active functional groups existing.[70] In addition, they can be easily synthesized using the recrystallization method. As the bipolar system, Na_2TP can access both positive and negative states from the neutral state. When used as the anode, each molecular unit can store two sodium ions at the sodiation potential of around 0.3 V versus Na^+/Na, thus achieving a capacity of around 250–300 mAh g^{-1} (Figure 13c).[70] Except for these small organic molecules, the organic building blocks with active functional groups can be polymerized to form polymers, metal–organic frameworks and covalent organic frameworks for sodium-ion storage.[71] However, organic anodes are suffering from the low electronic conductivity, short lifetime, and low volumetric energy density, which still need the contribution of conductive agents like carbon black or carbon nanotubes.[69]

In short, at the current stage of commercializing sodium-ion batteries, hard carbons from biomass are the most cost-effective choice of anode materials because of their low cost, enhanced sustainability, and suitable electrochemical performance compared with other insertion-type anode materials. For other insertion-type anodes, the utilization of hard carbons from biomass is also of vital importance to improve their inadequate electrical conductivities.

Alloying-Type: While insertion-type anodes, especially hard carbons, have shown satisfactory capacities for sodium-ion storage at the current stage, developing higher-energy anode materials beyond insertion for next-generation sodium-ion batteries is also very important in order to compete with lithium-ion batteries. Alloying anodes typically can provide ultrahigh capacities because one redox center is responsible for the multiple electron transfer, which belongs to the so-called "multielectron reaction" ($x\mathrm{Na}^+ + \mathrm{M} + x\mathrm{e}^- \leftrightarrow \mathrm{Na}_x\mathrm{M}$, M = alloying elements).[72]

As we know, metallic tin (Sn) and antimony (Sb) are the most investigated alloying anodes for sodium-ion storage (**Figure 14**a). Since each tin atom can combine with 3.75 sodium atoms, the high theoretical capacity of 847 mA h g^{-1} can be estimated with the resulting alloy of $Na_{15}Sn_4$ (Figure 14b).[74] The alloying of $Na_{15}Sn_4$ slowly happens at the potential of 0.21 V versus Na^+/Na.[75] However, pristine tin anodes usually go through a 4.2-fold volume expansion during the sodiation process, which leads to the continuous reconstruction of the SEI layer and the pulverization of the electrode.[74] Therefore, the Coulombic efficiency and lifetime of tin anodes are unacceptable. Furthermore, antimony anodes have a similar situation. Each antimony atom can alloy with 3 sodium atoms to form the hexagonal Na_3Sb phase with a calculated theoretical capacity of 660 mAh g^{-1}.[76] Nevertheless, antimony anodes also suffer from a huge volume expansion of 390% and sluggish reaction kinetics.[76] Meanwhile, the alloying potential of antimony is above 0.5 V versus Na^+/Na, which further decreases their energy densities.[76] Interestingly, the binary alloy of SnSb with decreased particle sizes can show enhanced structural stability based on reduced strain during the cycling testing, implying that the inherent properties including the particle size of alloys all affect the electrochemical performance.[77] Inspired

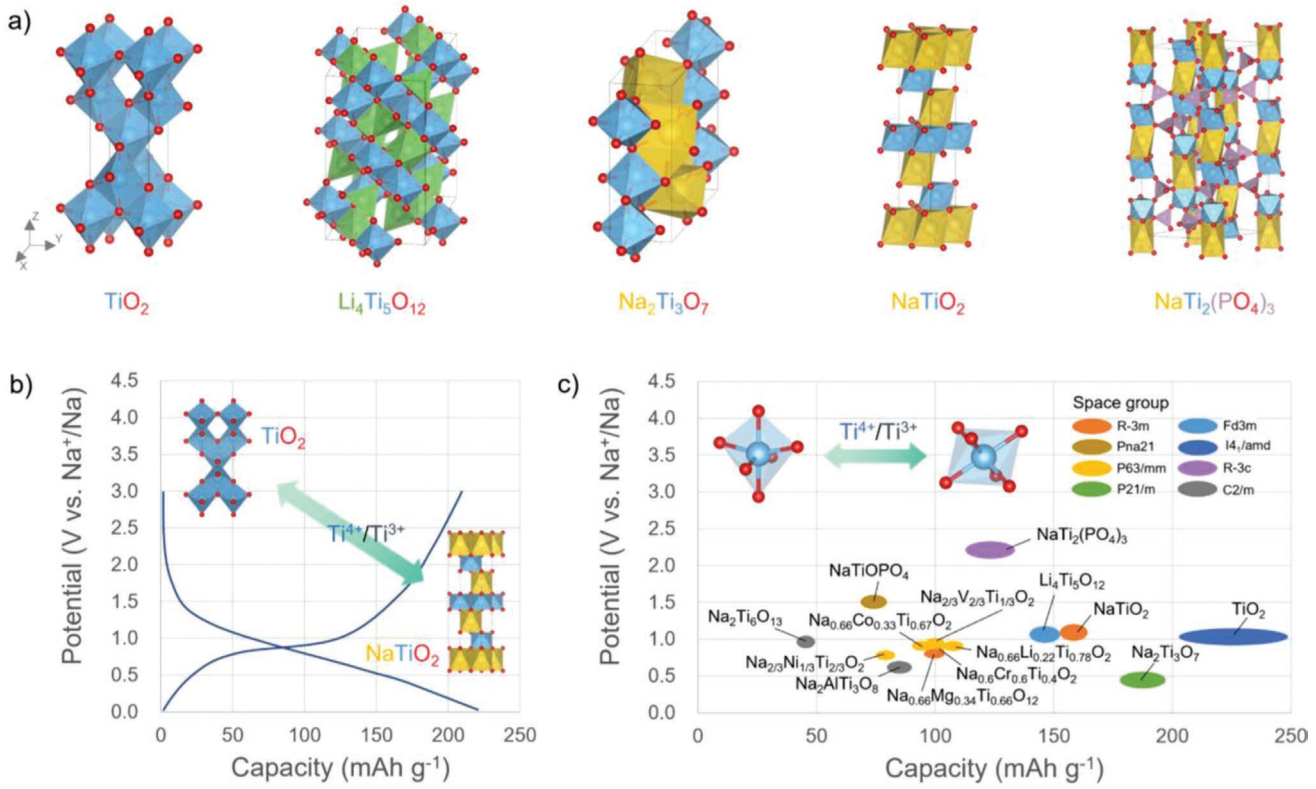

Figure 12. a) Crystal structures of titanate-based anode materials. b) Typical GCD curves of TiO_2 electrodes in the half configuration with the phase transformation between TiO_2 and $NaTiO_2$ during the sodiation and desodiation process. c) Summaries and comparisons of redox potentials and capacities of different titanate-based anode materials (data source collected from ref. [65]).

by this phenomenon, other metals can also be introduced into tin or antimony to form stable intermetallic compounds with suitable nanostructures and thus overcome the drawbacks of bare alloying-type anodes.[78] Besides, carbon nanomaterials like carbon nanotubes, carbon nanofibers, graphene, and carbon nanospheres have widely been employed as the matrix to allocate the volume expansion, avoid the agglomeration, and shorten the ion diffusion pathway, thus engineering the nanostructured alloying-type anodes with improved electrochemical performance.[79] Combined with additives of electrolytes such as fluoroethylene carbonate (FEC), the obtained fluorine-rich SEI layer can exhibit the great stability to cover the varied volumes of anode materials upon cycling.[80] However, the addition of expensive carbon nanomaterials or fluorine-containing electrolytes may decrease the cost-effectiveness of current sodium batteries, which needs a further eco-friendly modification of these systems.

As an abundant resource with environmental benignity, phosphorus (P) can also offer an impressive theoretical capacity of 2596 mAh g^{-1} for sodium-ion storage in comparison to metallic tin (Sn) and antimony (Sb) because one phosphorus atom can ideally combine with three sodium atoms to form Na_3P during the sodiation process (Figure 14d).[81] Meanwhile, the sodiation potential of phosphorus is around ≈0.3 V versus Na^+/Na, which can promise a broad working voltage in full cells.[81] In nature, there are three allotropes of phosphorus, including white phosphorus, red phosphorus and black phosphorus with different structural features (Figure 14c).[82] First, toxic white phosphorus exists in the molecular form of tetrahedral P_4, but it ignites in air at only around 50 °C, so it is not the best choice of anode materials.[82] Second, being prepared by the mild heating of white phosphorus, red phosphorus with a chain-like structure is more stable than white phosphorus.[39] Although commercial red phosphorus is very cheap, its low electronic conductivity significantly restricts its further application in batteries.[83] The last allotrope is black phosphorus, which can be made through the high-pressure heating of white phosphorus.[84] In the form of multiple stacked 2D layers, it is the most stable one from the point of view of thermodynamic.[84] Differing from the other two allotropes, black phosphorus is the semiconductor with a narrow bandgap of around 0.3 eV, thus offering a potential in the field of energy storage.[84] However, black phosphorus still suffers from the large volume changes during the charge–discharge process with a resulting unstable SEI layer and the electrode pulverization (Figure 14e).[73] By sandwiching the black phosphorus layer between graphene layers, the obtained hybrid electrode materials can exhibit high conductivity and stability with a reversible capacity close to 2500 mAh g^{-1}, but such kinds of nanoconstruction technologies still have a huge gap from large-scale applications at present.[73] Hence, efficiently combining sustainable carbons inspired by nature with alloying-type anode materials represents the more promising modification methods to enhance the electrochemical behaviors of alloying reactions in the near future.[19]

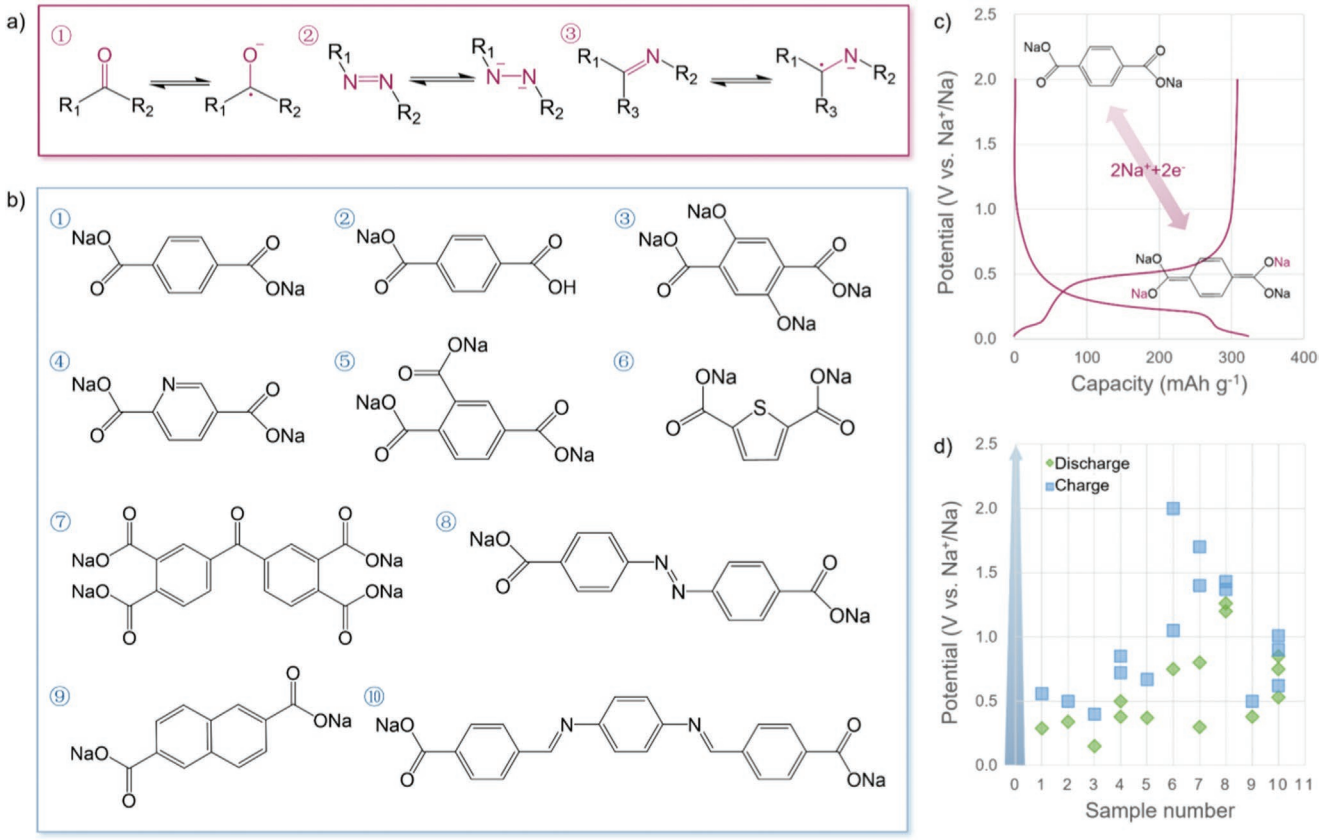

Figure 13. a) Schematically illustrating redox activities of organic moieties to interact with sodium ions. b) Molecular structures of redox-active organics for sodium-ion battery anodes. c) Typical GCD curves of Na_2TP in the half cell during the sodiation and desodiation process. d) Redox potentials of redox-active organics from (b) with different redox states (data source collected from ref. [69]).

Conversion-Type: Similar to the alloying-type anodes, conversion-type anode materials also store sodium ions based on the multielectron reactions. Most conversion-type anode materials are transition metal-based compounds of MN_x (M = transition metal elements, N = nonmetal elements like oxygen, sulfur, nitrogen, phosphorus, fluorine, etc.) (**Figure 15**a).[72] Based on the multiple electrons transferring with each transition metal ($MN_x + y\mathrm{Na}^+ + y\mathrm{e}^- \leftrightarrow \mathrm{M} + x\mathrm{Na}_{y/x}\mathrm{N}$), the reduction of conversion-type materials happens to form the two-phase materials where converted transition metal nanoparticles embedded in a $Na_{y/x}N$ matrix.[72]

Transition metal oxides represent the most classic conversion-type anode materials. Among various transition metals, earth-abundant iron (Fe) is a promising active redox center because of iron's variable valences. Therefore, the theoretical capacity of Fe_2O_3 anode materials is approaching 1000 mAh g^{-1} based on the redox pairs of Fe^{3+}/Fe^0.[88] According to the reported mechanism study, the sodiation of Fe_2O_3 anodes is a two-stage process with the reduction of Fe^{3+} into Fe^{2+} to form $Na_xFe_2O_3$ intermediate phases at the potential of around 0.8 V versus Na^+/Na, and then into Fe^0 to form Fe nanoparticles embedded in Na_2O matrix at the potential of around 0.4 V versus Na^+/Na (Figure 15b).[88] However, in practical applications, the reversibility of Fe_2O_3 anodes is limited by the low electronic conductivity, detrimental particle size, and sluggish sodiation kinetic.[86] In addition to Fe_2O_3, other transition metal oxides like Fe_3O_4, Co_3O_4, and CuO suffer from the similar challenges.[89] For example, even coupling with carbon nanomaterials, nanostructured electrode design or FEC additives, the reversible capacity of Co_3O_4 is still much lower than its theoretical capacity of 890 mAh g^{-1}.[90] With a large ionic radius of sodium ions, extracting sodium ions from the insulated Na_2O matrix is thermodynamically unfavorable and thus decreases the Coulombic efficiency of each sodiation and desodiation process of these transitional metal oxide anodes.[89] Therefore, transitional metal chalcogenides, especially sulfides, are considered to be the more promising anode materials than oxides on account of the higher conductivity of formed Na_2S and the weaker chemical bonding between transitional metal and sulfur.[91] Except for traditional transition metal chalcogenides such as cubic FeS_2, there are other types of transition metal chalcogenides with layered structures, including MoS_2, $MoSe_2$, WS_2, and VS_2.[92] The layers within this kind of chalcogenides are interacted with each other through the weak van der Waals force, enabling the better ion diffusion between layers.[92] Meanwhile, the sodium-ion storage mechanism of layered chalcogenides differs from FeS_2. Taking MoS_2 as an example, the Na_xMoS_2 phase ($x < 2$) will be firstly formed by the intercalation of sodium ions into the layered structures at the potential above 0.4 V versus Na^+/Na.[93] With the sodiation process continuing at the potential below 0.4 V versus Na^+/Na, the Na_xMoS_2 phase

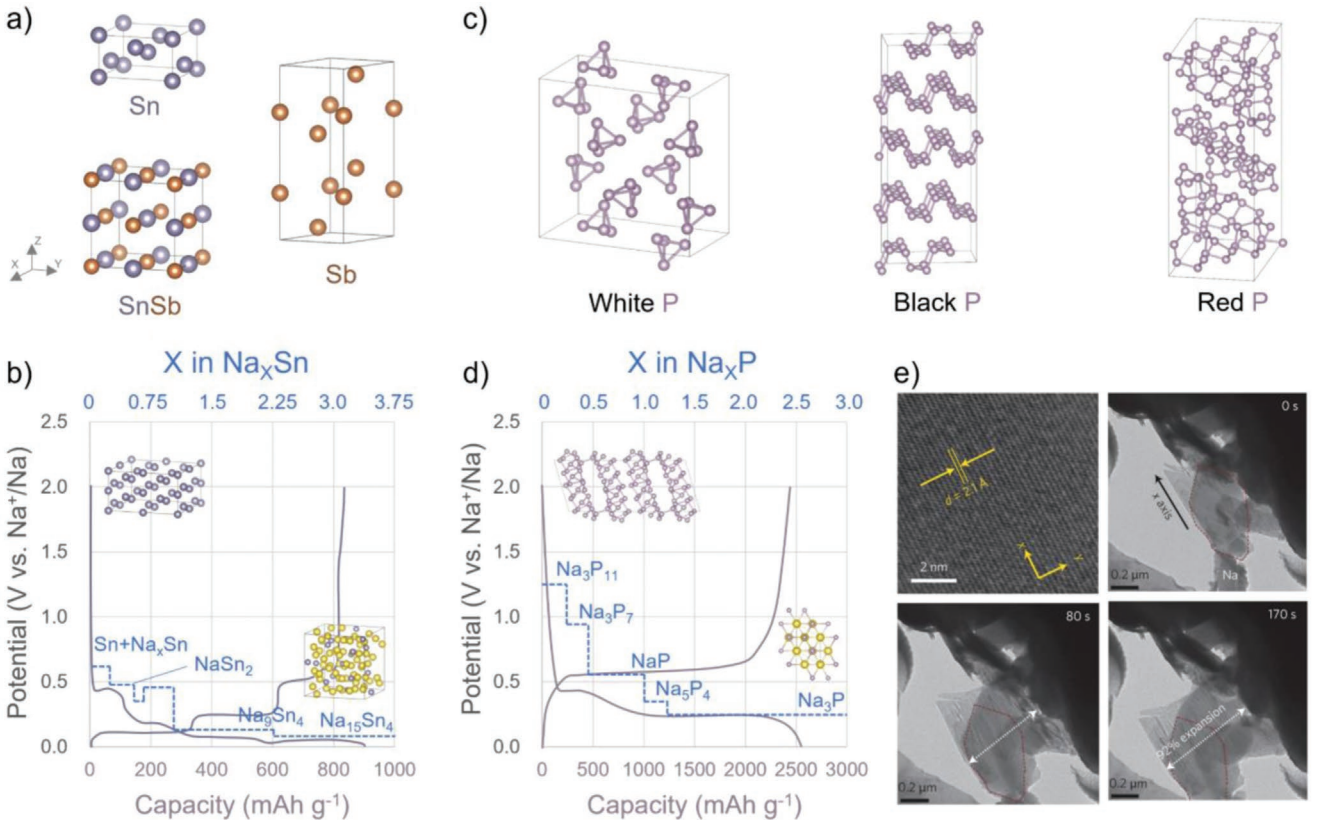

Figure 14. a) The crystal structures of tin, antimony, and their alloys of SnSb. b) The typical GCD curves of tin anode materials for sodium-ion storage with the corresponding phase transformation stages at specific potentials. c) The molecular structures of three allotropes of phosphorus. d) The typical GCD curves of phosphorus-based electrode for sodium-ion storage with the corresponding phase transformation stages at specific potentials. e) In situ TEM images of black phosphorus illustrating its layer-by-layer structure and the volume expansion during the sodiation process. Reproduced with permission.[73] Copyright 2015, Springer Nature.

is transformed into metallic molybdenum (Mo) embedded in Na_2S.[93] When incorporated with conductive carbons, the nanostructured MoS_2 reported in the literature can deliver a specific capacity of 854 mAh g^{-1} (0.1 A g^{-1}).[94] Nevertheless, the formed intermediate products such as polysulfides are soluble in nonaqueous electrolytes, which means during the cycling, the reversibility and lifetime of anodes still encounter challenges.[94] Furthermore, transition metal nitrides, phosphides, and fluorides such as VN, CoP, and FeF_2 have also been explored as conversion-type anode materials.[89] Indeed, conversion-type anode materials can exhibit electrochemical activity to store sodium ions, but the fundamental understanding of the complexly formed intermediate phases during the discharge–charge process is still needed to guide the rational design of nanostructured electrodes with enhanced electrochemical performance. Additionally, from the reported cases, the importance of carbon materials can be observed for conversion-type anodes to improve the electronic conductivity and stabilize the structural changes.[87]

If the transition metal elements in conversion-type oxides or sulfides are located in Groups IV and V that can further alloy with sodium ions, the conversion–alloying anode materials can be achieved including SnO_2, SnS_2, Sb_2O_3, and Sb_2S_3.[95] Due to the higher redox potentials, conversion reactions happen first during the sodiation process to obtain the transition metal nanoparticles.[85] At the lower potentials, sodium ions alloy with the reduced transition metals to deliver a higher sodium-ion capacity.[85] The formed Na_2O or Na_2S matrix can allocate the volume change derived from the alloying reaction as well as alleviate the agglomeration of anode materials upon cycling to some extent.[85] However, as a combination of previously mentioned alloying- and conversion-type anodes, the sluggish kinetics of these two reactions based on sodium ions still result in the limited rate performance of these conversion–alloying anode materials.[96] Carbon materials with the good conductivity and mechanical properties are suitable additives to accelerate and stabilize the electrochemical behaviors of both alloying and conversion reactions.[96] The summaries of reaction potentials and specific capacities of different conversion-type anodes are shown in Figure 15c.[97]

Metallic Sodium Anodes: Compared to the above-mentioned anode materials, metallic sodium is actually the original and ultimate anode material for sodium-ion storage because of its high theoretical capacity of 1166 mAh g^{-1} and the lowest redox potential based on the redox pair of Na^+/Na.[53] At the very beginning of sodium battery development, metallic sodium is the initial choice of anodes, but the major problem of sodium metal anodes is the dendrite formation derived from the random nucleation and deposition processes of metallic sodium (**Figure 16**a).[11] The formation of sodium dendrites

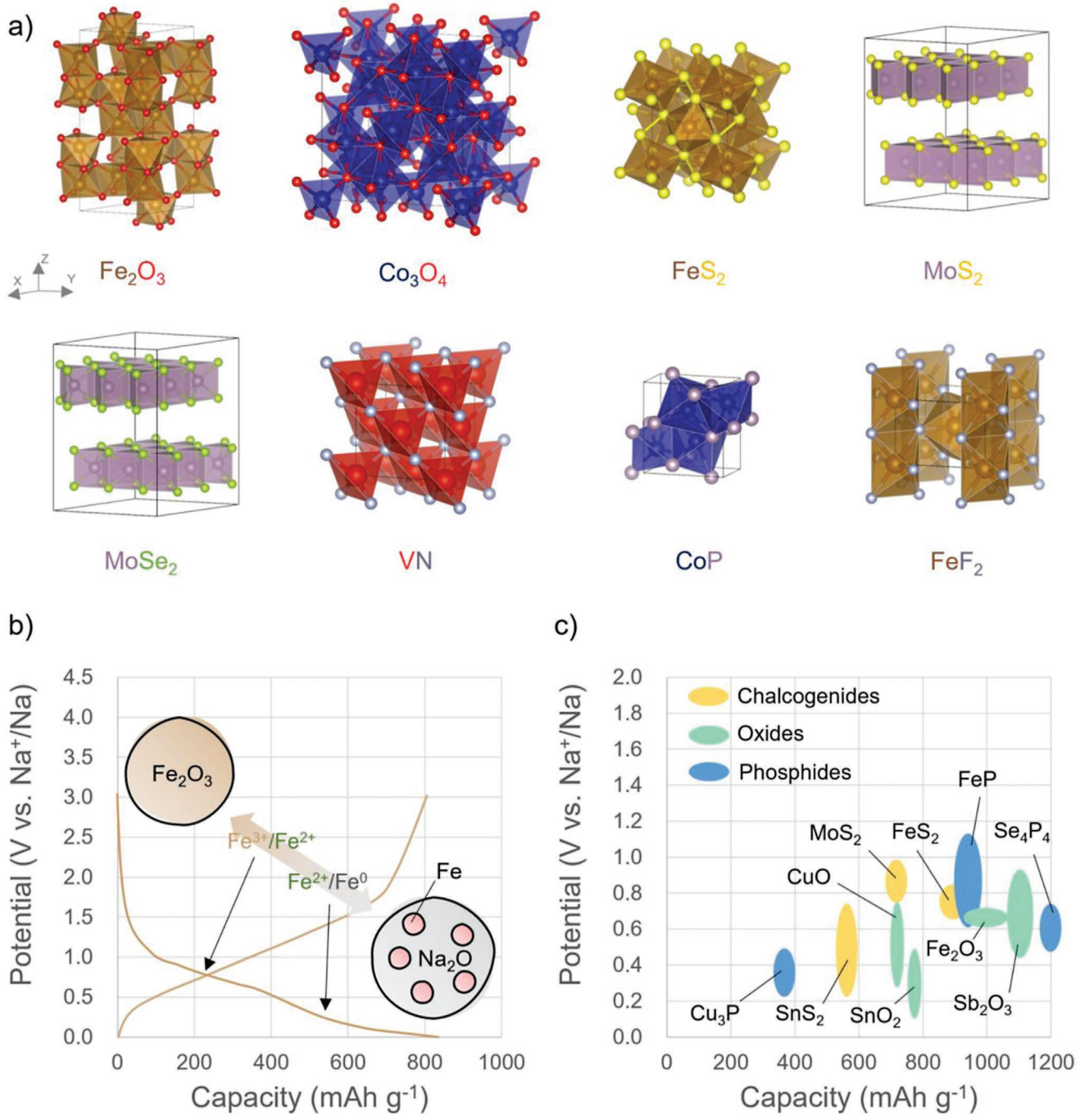

Figure 15. a) The crystal structures of typical conversion-type anode materials. b) The typical GCD curves of Fe_2O_3 anodes for sodium-ion storage with the schematic illustrations of the two-stage phase transformation based on the redox pairs of Fe^{3+}/Fe^{2+} and Fe^{2+}/Fe^0 during the sodiation process. c) The summaries of reaction potentials and specific capacities of different conversion-type anodes (data source collected from refs. [85–87]).

can lead to excessive inactive sodium upon cycling because of the continuous crack and reconstruction of the SEI layer under the large volume variation of metallic sodium, which decreases the reversibility of the sodiation and desodiation process (Figure 16b).[12] Furthermore, the lifetime of battery cells is restricted by the short-circuiting after the sodium dendrites penetrate the separator.[12] To avoid such challenging issues in the efficiency and safety of metallic sodium, scientists abandoned metallic sodium and turned to developing host materials to store sodium ions more stably based on the "rocking-chair" mechanism before. However, with the development of battery technologies using the electrolyte engineering, interface engineering, solid-state electrolytes or versatile functional hosts, the aim to revive the metallic sodium anode for high-energy sodium batteries is attracting wide attention from the battery community again (Figure 16c).[11]

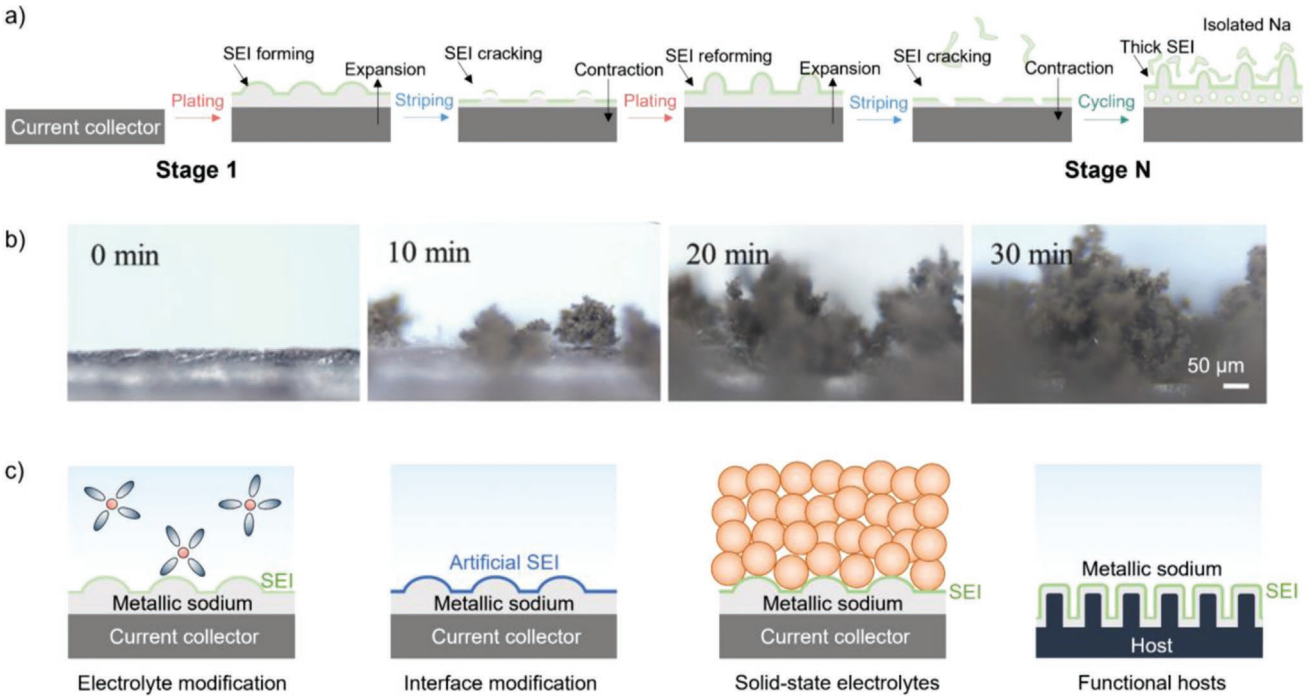

Figure 16. a) Schematic illustrations of the sodium plating and stripping processes upon cycling. b) Optical microscopy images of the sodium dendrite formation during the metallic sodium deposition in carbonate-based electrolytes. Reproduced with permission.[98] Copyright 2017, Wiley). c) Schematic illustrations of strategies to suppress the dendrite formation and stabilize the sodium metal anodes.

First of all, the electrolyte modification has been widely used to improve the stability of metallic sodium anodes. Traditional carbonate-based electrolytes like 1 M $NaPF_6$ in the mixed solvent of ethylene carbonate (EC) and dimethyl carbonate (DMC) (1:1 in volume) during the reduction and decomposition will form the SEI layer composed of the mixture of organics such as sodium alkyl carbonates and inorganics including Na_2CO_3 and Na_2O.[99] This kind of SEI layer is brittle and fragile with heterogeneous ion conductivities, which can cause the inhomogeneous ion flux and thus form the uncontrollable sodium dendrites during the continuous plating and stripping process.[99] Therefore, additives like fluorinated compounds have been used to increase the amount of sodium fluoride in the SEI layer and thus densify the SEI layer.[99] However, the most fluorinated additives such as hydrofluoric acid (HF) are toxic and harmful to human beings and environments. Except for carbonate-based electrolytes, ether-based electrolytes are also the choice to stabilize sodium metal anodes, which is attributed to the formation of flexible organic-dominated SEI layers.[33] The limitations of ether-based electrolytes are still obvious because they are easier to be decomposed under the low anodic potentials (≈4 V vs Na^+/Na), thus decreasing the working voltage windows and safety of the full cells.[33] Another choice to suppress sodium dendrites is the utilization of high-concentration electrolytes.[100] When the concentration of electrolytes is high enough to have limited free solvent molecules, sodium ions cannot be fully solvated by solvent molecules and thus become favorable for fast ion transfer,[101] which can increase the critical current needed for nonuniform metallic deposition. Nevertheless, the high cost of high-concentration electrolytes is not ideal for the commercialization of sodium metal batteries.[102]

The interface modification like the artificial SEI layer can also be used to stabilize sodium metal anodes. The most classic protective and ionic conducting layer is the Al_2O_3 nanolayer coated by atomic-layer deposition (ALD), which not only mechanically alleviates the sodium dendrite formation but also delays the corrosion of sodium metal anodes both in air and in electrolytes.[103] The main disadvantage of advanced coating methods for thin films is their high expense at the industry level.[103]

Since solid-state electrolytes can physically suppress the sodium dendrite growth,[104] the development of solid-state electrolytes is also of great importance to obtain sufficient mechanical and electrochemical properties for sodium metal batteries. In addition, the interface between electrodes and electrolytes needs to be improved to decrease the polarization within solid phases.[104] Solid-state electrolytes can be categorized into three main kinds including inorganic ceramics, organic polymers, and inorganic–polymer composites.[105] In general, inorganic ceramics such as sodium-containing oxides, sulfides, nitrides, and phosphates show suitable ionic conductivity ranging from 0.1 to 10 mS cm^{-1} at the room temperature and appropriate mechanical properties varying from 10 to 200 GPa.[35] However, their poor adhesion with sodium metal anodes can increase the interface resistance and thus limit the fast-charge performance of sodium metal batteries.[35] In addition, oxides are usually obtained by the high-temperature sintering based on huge energy consumptions, while the limited electrochemical stability window of sulfides usually induces the side reactions within sodium metal batteries.[35] By contrast, the interface between solid polymer electrolytes and sodium metal anodes is more adhesive and

compact, but their ionic conductivity (0.001–0.1 mS cm^{-2} at 25 °C) and mechanical properties (≈0.1 GPa) seem to be unsatisfactory.[106] Hence, the inorganic–organic composite electrolytes are an essential option for stable sodium metal anodes. For instance, a polymer/ceramic/polymer sandwich structure can be employed to solve the dilemma between mechanical/electrochemical properties and interface contact.[107] More efforts are still needed to further enhance the performance of solid-state electrolytes, thus achieving the high-energy solid-state sodium batteries with sodium metal anodes.

Last but not least, functional hosts to accommodate sodium metal anodes are one of the most promising methods for stable sodium metal batteries. An efficient host can induce the uniform metallic sodium deposition by regulating the homogeneous energy transferring and ion flux.[108] In addition, the volume changes can be accommodated in functional hosts by dividing dense sodium metal anodes into smaller sodium clusters.[109] Therefore, the sodium dendrites can be alleviated when the even metallic deposition process is controlled. Excellent sodiophilicity of the host materials with uniformly disturbed nucleation sites on the surface is essential.[110] Numerous substrates with 3D structures have been employed to act as the function host for sodium metal anodes.[111] However, most commercial substrate materials like copper and aluminum lack good wettability with metallic sodium.[112] Therefore, surface functionalization methods are usually used to modify those functional hosts, including the growth of ZnO nanorods on their surfaces which can increase the sodiophilicity and act as the nucleation sites of metallic sodium.[112] In this situation, versatile carbon materials with better sodiophilicity and natural nucleation sites like oxygen functional groups can be another good choice for functional hosts.[113] For example, the reduced graphene oxide can be used as the matrix to stabilize sodium metal anodes.[114] The obtained reduced graphene oxide/metallic sodium composite anodes can exhibit an improved lifetime and less polarization.[114] The next step is to develop high-performance, low-cost, and sustainable carbon hosts for sodium metal anodes, which is promising for the application of next-generation sodium metal batteries.[115]

To sum up, according to the critical insight into the fundamentals, status, and promise of all types of anode materials, the utilization of sustainable carbons inspired by nature is probed to be indispensable to anode materials as not only the active material directly to store sodium ions but also the functional host or additive to stabilize other anode materials. At the current development stage, sustainable carbons have obvious advantages such as appropriate capacity, high safety, excellent stability, and low cost compared to other types of anode materials (**Figure 17**). That is to say, sustainable carbons have the biggest promise to be applied in the large-scale production of sodium batteries. Of course, other types of anode materials, especially high-energy metallic sodium anodes, also exhibit their specific advantages and disadvantages in terms of performance and cost-effectiveness (Figure 17), which deserves more effort from scientists to improve their stability in the future. Detailed comparison and evaluation of different types of anode materials based on performance and cost-effectiveness are shown in Figure 17.

2.2.2. Cathodes

In accordance with the literature analysis, the most promising cathode materials for sodium batteries can be respectively grouped into three main families which are layered oxides, polyanionic compounds, and Prussian blue analogs.[23] Except for the three main families based on the intercalation/insertion mechanism, advanced sulfur or oxygen cathodes based on redox reactions of polysulfides or oxygen gas can be coupled with sodium metal anodes to achieve higher energy densities.[116,117]

Intercalation-Type: The sodium-based layered oxides (Na_xMO_2) usually consist of one or more kinds of (transition) metals noted as M (e.g., Fe, Mn, Ni, Ti, Co, Al, Cu, etc.).[120] According to the different coordinate types of sodium atoms, the layered oxides can be divided into octahedral or prismatic types.[120] In addition, depending on how the stacking arrangement of layers repeats, the octahedral- or prismatic-type layered oxides can be further sorted into O2 (P2) or O3 (P3) types (**Figure 18**a).[120] The sodium atoms are stored between the metal oxide layers based on the redox pairs of metals. In a normal situation, layer oxides can have a specific capacity ranging from 100 to 200 mAh g^{-1}, with an average working potential between 2.5 and 3.5 V versus Na^+/Na (Figure 18d,e).[121] One of the challenges of layered oxides is the structural degradation during cycling, which can cause the loss of reversible capacity.[121] Hence, the introduction of other transition metals to reconstruct the crystal structure is meaningful. For instance, titanium (Ti) and nickel (Ni) were introduced into $Na_{0.9}Cu_{0.22}Fe_{0.30}Mn_{0.48}O_2$ to form $Na_{0.9}Cu_{0.12}Ni_{0.10}Fe_{0.30}Mn_{0.43}Ti_{0.05}O_2$,[122] thus manipulating the originally unfavorable phase transformation. On the other hand, although the existence of titanium (Ti) and nickel (Ni) components within the structure can increase the reversible capacity and working potential, titanium (Ti) and nickel (Ni) as critical elements in the battery industry usually challenges the overall cost and sustainability of cathodes materials for sodium batteries.[121] Therefore, the employment of earth-abundant elements like iron (Fe) and manganese (Mn) to fabricate the high-performance and low-cost cathode materials is also important for sodium batteries. For example, Yabuuchi et al.[123] prepared a P2-type $Na_{2/3}Fe_{1/2}Mn_{1/2}O_2$ without cobalt (Co) or nickel (Ni), thus achieving a specific capacity of 190 mAh g^{-1} and an average working potential of 2.75 V versus Na^+/Na. Moreover, the MO_6 octahedra composed of M–O bonds with covalent character exists in the layered oxides, where the changes of the valence of oxygen element (O) can happen based on the redox pairs of O^{2-}/O.[124] Such a kind of anionic redox behavior in layered oxides at high potentials can enhance the sodium-ion storage capability and energy density.[125] Nevertheless, the oxidation of oxide ions, along with the release of O_2 on the surface, usually triggers the permanent structural reconstruction of layered oxides, inducing the irreversible loss of high-potential capacity.[126] Strategies to cage O_2 within the bulk phase of layered oxides for reversible redox reactions can avoid the structural instability.[126] House et al.[127] found that the ribbon-ordered superstructure in $Na_{0.6}[Li_{0.2}Mn_{0.8}]O_2$ can overcome the migration of transition metals and promote stable electron holes on O^{2-} to reduce the hysteresis during the first cycle. Besides, the electron and ion diffusivities are limited in layered oxides, so combined with carbon materials, the electrode architecture strategies like

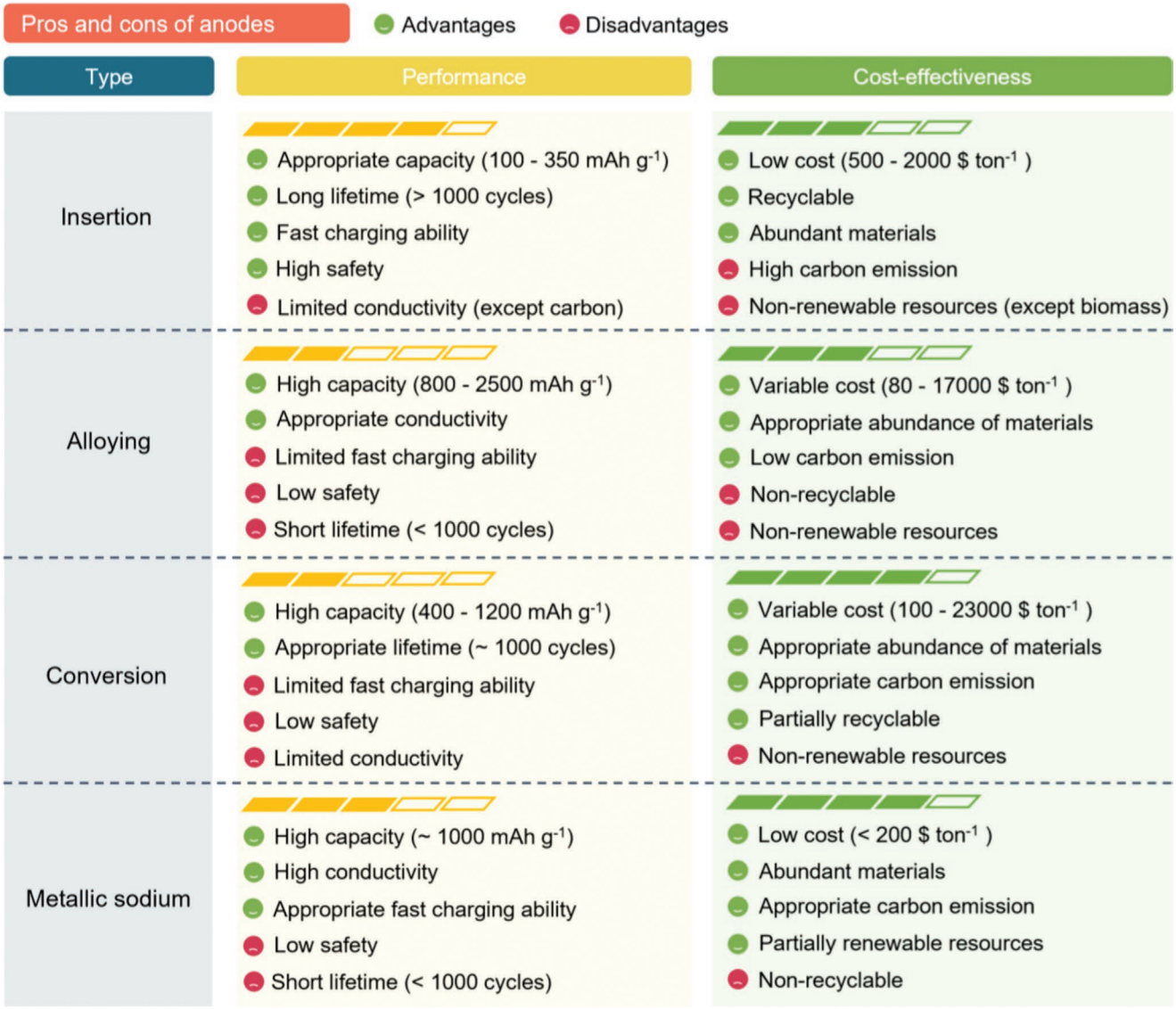

Figure 17. Comparisons of pros and cons of various anodes on aspects of performance and cost-effectiveness.

nanocarbon material coating are often used to enhance the electrical and ionic conductivity, which can provide potential routes for high-energy cathodes.

Similar to layered metal oxides, polyanionic compounds are composed of the transition metal (e.g., V, Mn, Fe, Co, etc.) with the anion (e.g., PO_4^{3-}, $P_2O_7^{4-}$, SO_4^{2-}, SiO_4^{4-}, F^-, etc.) to store sodium ions through the redox reaction of the transition metal (Figure 18b).[128] Compared to layered metal oxides described above, polyanionic compounds usually possess the higher redox potentials ranging from 3.0 to 4.0 V versus Na^+/Na (Figure 18d), because the existence of anionic centers with increased electronegativities can delocalize the electron from the bonds between transition metal atoms and oxygen atoms to decrease the reactivity of transitional metals.[128] Such a kind of inductive effect of polyanionic compounds affects the redox potentials of transitional metals, which is beneficial to the increase in working voltages of full cells using polyanionic compound cathodes.[129] However, the molar mass of polyanions is usually higher than that of oxide ions when coupled with the similar number of transitional metal atoms, thus resulting in the decrease in the specific capacity of polyanionic compounds to around 100 mAh g^{-1} (Figure 18e).[129] Furthermore, unlike the layered oxides with the ordered layer structures which can facilitate the chemical diffusivity, the ion and electron diffusions within polyanionic compounds are further restricted by their intrinsic crystal structures to some extent.[128] Hence, there are two common strategies to enhance the chemical diffusivity of polyanionic compounds: one is the carbon coating of the particles, and the other is decreasing the particles of compounds to the sub-micrometer level.[130] Until now, NASICON-type $Na_3V_2(PO_4)_3$ has been considered to be the most classical polyanionic compound cathode for sodium batteries due to its satisfactory reaction kinetics, the acceptable capacity of around 110 mAh g^{-1} and the outstanding average working potential of around 3.4 V versus Na^+/Na (Figure 18e).[119] Similar to the commercial $LiFePO_4$ cathode for lithium batteries, the desodiation

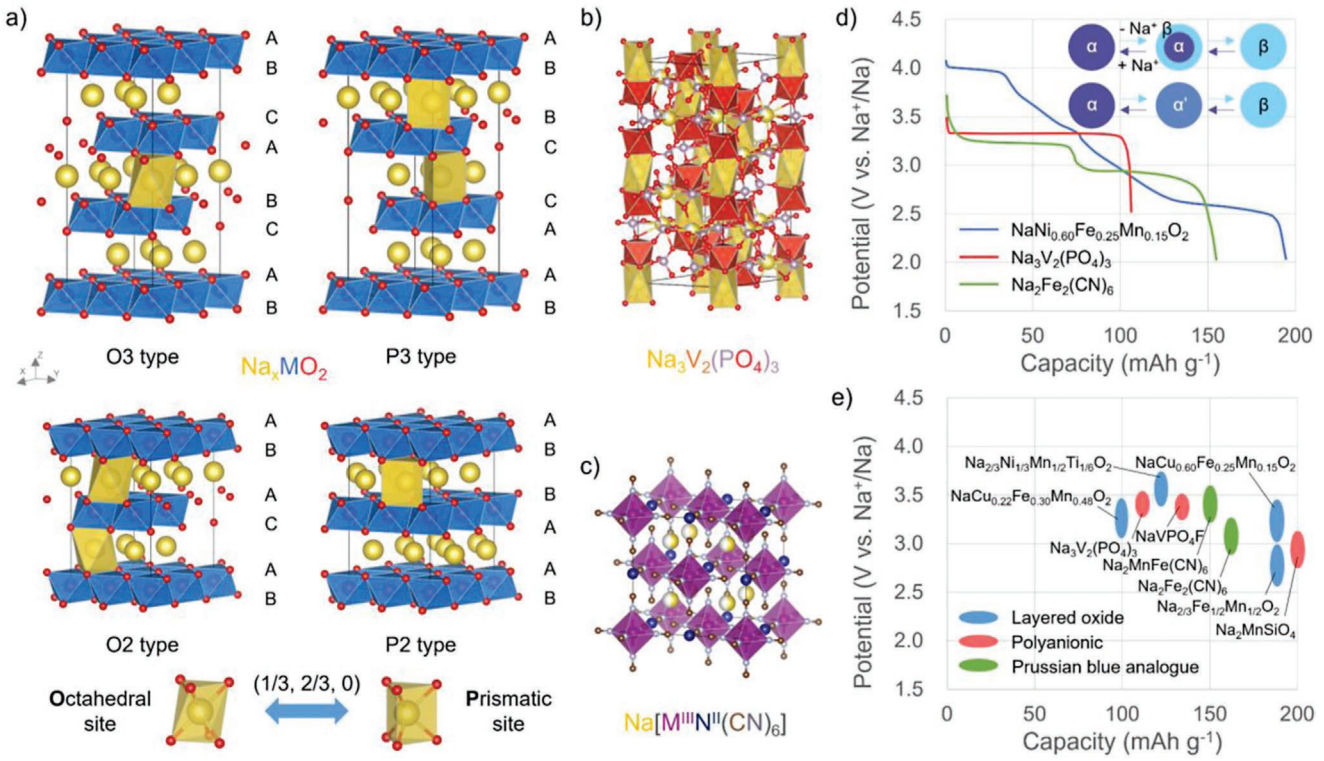

Figure 18. Typical crystal structures of a) layered oxides, b) polyanionic compounds, and c) Prussian blue analogs. d) Typical discharge curves of layered oxides, polyanionic compounds, and Prussian blue analogs with the schematic illustrations of single- and two-phase reactions. e) Comparison of average working potentials and capacities of different sodium cathode materials (data source collected from refs. [23,118,119]).

and sodiation of $Na_3V_2(PO_4)_3$ cathode belong to the two-phase reaction with a plateau redox potential.[119] More efforts are still needed to further increase the capacity and rate performance of polyanionic compounds, such as developing the high-performance Na_2MnSiO_4 cathode with a specific capacity of around 200 mAh g^{-1}.[131]

Prussian blue (PB) and its analogs are a family of perovskite-type compounds mainly in the form of $Na_xM[M'(CN)_6]\cdot nH2O$, where M and M′ are both transitional metals (e.g., Fe, Co, Ni, Mn, Cu, Zn, etc.) (Figure 18c).[118] Through the two-electron redox reactions of transitional metals, Prussian blue analogs can achieve a high capacity of sodium-ion storage usually ranging from 150 to 200 mAh g^{-1} as per molecular unit can store two sodium ions during the potential range between 3.0 and 3.5 V versus Na^+/Na (Figure 18d,e).[118] Meanwhile, their open-framework, cubic crystal structures can allow the more rapid sodium-ion insertion and extraction with the minimal structural change than conventional insertion-type layered metal oxides, thus ensuring their excellent rate and cycling performance.[132] Differing from the complex synthesis methods of layered metal oxides and polyanionic compounds involving the ball milling and high-temperature sintering, Prussian blue analogs can be synthesized and tuned using a lost-cost and convenient coprecipitation reaction of variable precursors in the aqueous system.[132] However, the coordinated water in the lattice of Prussian blue analogs highly retained from this facile synthesis method can decrease their electrochemical stability under high potentials and reduce their specific capacity, as the coordinated water not only diffuses to the organic electrolyte but also occupies the interstitial spaces of Prussian blue analogs.[133] Therefore, decreasing the coordinated or interstitial water content and increasing the crystal quality of Prussian blue analogs are very important but challenging for achieving outstanding electrochemical performance. The vacuum drying of as-prepared samples such as $Na_2MnFe(CN)_6$ at 100 °C for 30 h can eliminate the interstitial H_2O to some extent, which was found by Song et al.[134] Furthermore, making use of this feature of Prussian blue analogs, Jiang et al.[135] also employed them as the cathode materials for some aqueous batteries, which can avoid the drawbacks of coordinated water. Last but not least, Prussian blue analogs have the potential toxicities because of the possible cyanide releasing at high temperatures or under ultra-acidic conditions, which needs more assessments on this issue.[118]

Sulfur and Oxygen Cathodes: As metallic sodium is considered to be the ultimate choice of the anode for sodium batteries, scientists are keen to develop suitable cathode materials that can couple with metallic sodium. In this situation, sulfur and oxygen can also be the ideal cathode choices.[136] First, when the abundant sulfur is applied as the cathode material (**Figure 19**a), the theoretical specific capacity can reach as high as 1675 mAh g^{-1}, and the energy density of obtained room-temperature sodium–sulfur (Na–S) batteries can be 1274 Wh kg^{-1} (Figure 19b).[137] Different from the previously discussed cathode materials, sulfur stores sodium ions based on the conversion mechanism with the formation of Na_2S_x rather than the intercalation/insertion mechanism.[138]

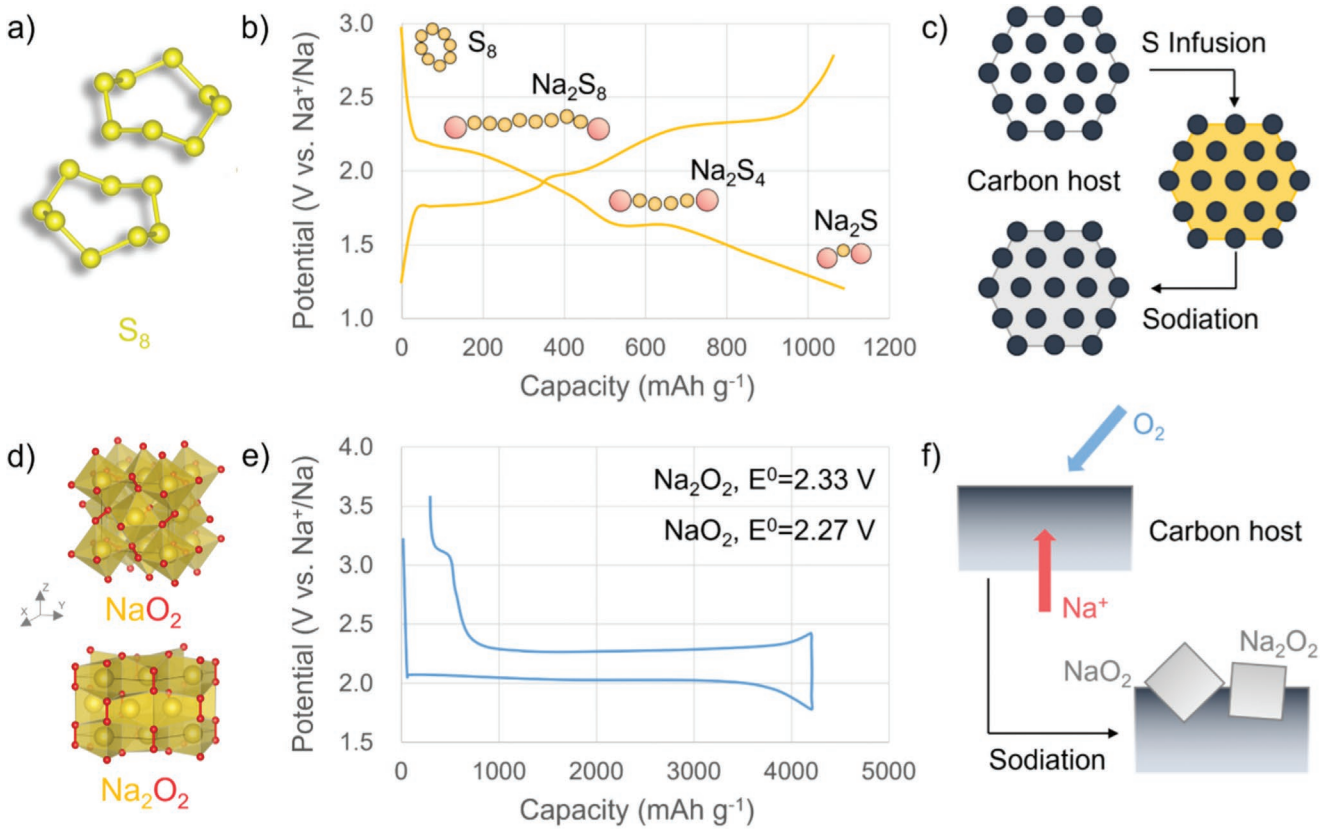

Figure 19. a) Structural illustration of sulfur. b) Typical discharge–charge curve of sulfur cathodes for sodium-ion storage. c) Schematic illustration of functional carbon hosts for the protection of sulfur cathodes. d) Crystal structures of NaO_2 and Na_2O_2. e) Typical discharge–charge curve of oxygen cathode for sodium-ion storage. f) Schematic illustration of functional carbon hosts for oxygen reduction and evolution reactions.

However, since the active sulfur is nonconductive, it suffers from sluggish electrochemical reaction kinetics, and the huge volume change of sulfur during the sodiation and desodiation process can cause the severe collapse of the cathode.[138] In addition, the high solubility of intermediate compounds, namely, the sodium polysulfides such as Na_2S_8 and Na_2S_4, can diffuse to the anode side and react with metallic sodium to decrease the reversibility of its sodium-ion storage capacity, which is called the "shuttle effect."[138] Compared with sulfur cathodes, oxygen cathodes are facing the similar situation. The theoretical energy densities of sodium–oxygen (Na–O_2) batteries can reach 1602 and 1105 Wh kg^{-1}, respectively, according to the formed Na_2O_2 and NaO_2 (Figure 19d,e).[117] Nevertheless, the slow kinetics of the redox reactions of oxygen including the oxygen reduction and evolution reactions (ORR and OER) can increase the overpotential and decrease the rate performance of sodium–oxygen batteries.[139] Also, oxygen cathodes have the mass transport problems because the formed Na_2O_2 and NaO_2 will block the pathways for oxygen gas and electrolytes.[139] To solve these challenges of sulfur and oxygen cathodes, carbon materials have been widely used as the versatile functional hosts for them because of their high conductivity, hierarchical pore structures, and active sites possibly from embedded electrocatalysts.[140,141] For sulfur cathodes, carbon functional hosts can restrict the volume change and avoid the "shuttle effect" of polysulfides to some extent (Figure 19c).[140] For oxygen cathode, carbon functional hosts can accommodate the formed oxides and ensure the pathway for continuous oxygen redox reactions (Figure 19f).[141] The high conductivity of carbon functional hosts and the embedded electrocatalysts can decrease the polarization and provide active sites to reduce the energy barriers of electrochemical reactions.[141] The development of both sulfur and oxygen cathodes are in their infancy era, which needs more efforts to fabricate high-performance, low-cost, and sustainable carbon functional hosts for them.

To sum up, since most cathode materials are nonconductive, the introduction of carbon materials as additives, coating layers or functional hosts is useful and essential for cathode materials. Hence, developing sustainable carbon materials inspired by nature shows great necessity not only for anode materials but also for cathode materials to achieve excellent electrochemical performance. Based on the pros and cons of cathode materials (**Figure 20**), intercalation-type cathode materials with both appropriate capacity, lifetime, and cost-effectiveness become the promising choice for the industry-level fabrication of sodium batteries at the current stage. However, toward next-generation sodium batteries with improved performance and enhanced sustainability, the development of high-performance oxygen or sulfur cathodes, coupled with stable sodium metal anodes, deserves more effort from the energy storage community (Figure 20). Detailed comparison and evaluation of

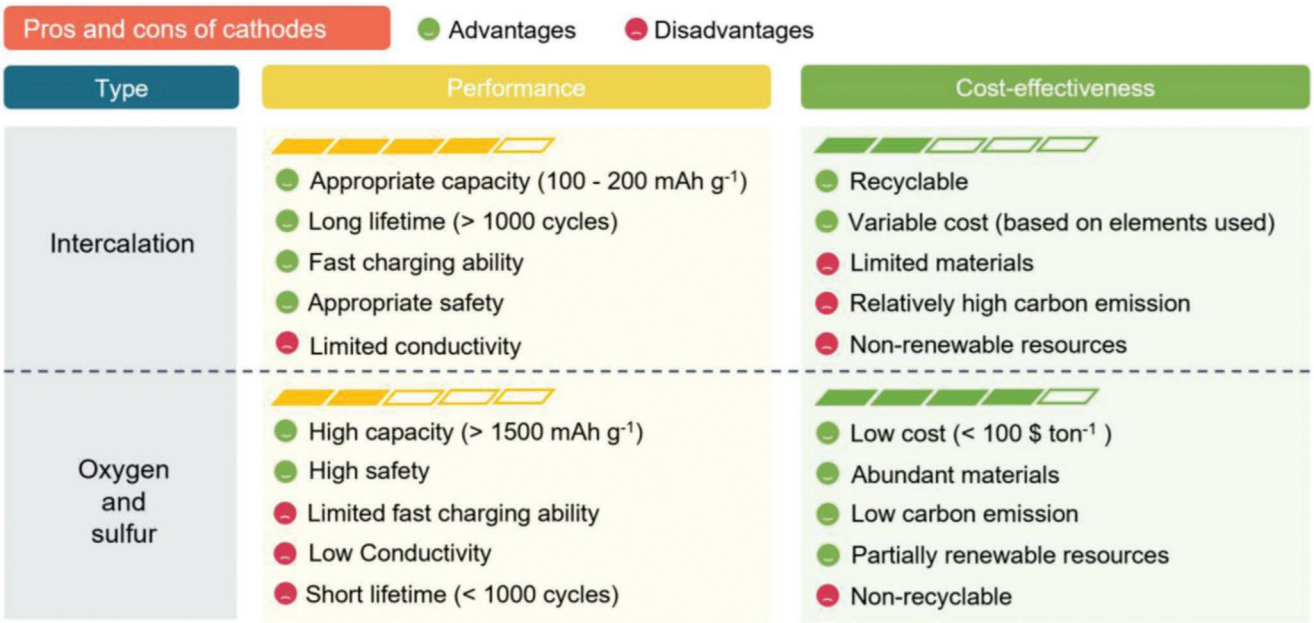

Figure 20. Comparisons of pros and cons of various cathodes on aspects of performance and cost-effectiveness.

different types of cathode materials based on performance and cost-effectiveness are shown in Figure 20.

2.2.3. Electrolytes

The literature survey shows that research on electrolytes seems to be neglected currently for sodium batteries. In fact, the conversion of electrolytes from liquid to quasi solid and all solid states is of great necessity and challenge.

Liquid Electrolytes: For conventional sodium batteries, especially sodium-ion batteries, the most common choice of the electrolyte is 1 M sodium salts (e.g., $NaPF_6$, $NaClO_4$, NaTFSI, $NaCF_3SO_3$, etc.) in carbonate-based nonaqueous solvents (e.g., EC, PC, DMC, DEC, EMC or a mixture of these solvents, etc.) because of its excellent ionic conductivity (≈1–10 mS cm^{-1}), suitable cost-effectiveness and outstanding electrochemical stability (up to around 4.5 V vs Na^+/Na) (**Figure 21**a),[142] which is very similar to current commercial lithium-ion batteries based on host materials for lithium-ion storage. At the salt concentration of 1 M, the ionic conductivity often reaches its maximum value.[142] When the salt concentration decreases, the cost and viscosity of electrolytes can be reduced at the same time, but the ionic conductivity usually decreases a lot as well.[143] By contrast, a higher salt concentration can reduce the free solvent molecules and shorten the ion diffusion pathway, which can broaden the electrochemical stability window and benefit the high-rate performance.[144]

As mentioned above, the SEI formed during the reduction of carbonate-based electrolytes is composed of the brittle and fragile mixture of organics (e.g., sodium alkyl carbonates, etc.) and inorganics (e.g., Na_2CO_3, Na_2O, etc.) with heterogeneous ion conductivities, which may be not suitable for alloying anodes or sodium metal anodes. In this situation, fluorinated additives (e.g., HF, FEC, etc.) or glycol ether solvents (e.g., DME, diglyme, etc.) can be employed to form the dense and flexible SEI layers (Figure 21a).[99] According to the literature, the SEI layer in the presence of FEC turns into a multilayer structure rather than the mosaic model, in which the inner layer is the organic matrix, while the outside layer is sodium oxides.[145] In addition, the SEI layer derived from glycol ether solvents mainly consists of oligomers.[146] However, ether-based electrolytes have the lower anodic decomposition potential and lower ionic conductivity than carbonate-based electrolytes when the salt concentration is similar.[146]

Compared to organic electrolytes with high flammability, aqueous electrolytes with a better safety are also attracting interest from scientists.[102] To overcome the limited electrochemical stability of aqueous electrolytes, one strategy is to develop electrode materials that can work within the redox potential range of aqueous electrolytes, and the other is the utilization of "water-in-salt" electrolytes with an ultrahigh salt concentration (usually around 20 M) which can diminish the free solvent molecules and thus avoid the decomposition of aqueous electrolytes.[101] Nevertheless, similar to the high-concentration organic electrolytes, the high cost of "water-in-salt" electrolytes, the high-quality requirement of salts and solvents as well as the salt precipitation problems are all challenging for scientists, which needs more effort to develop low-cost, stable, and high-performance aqueous batteries.[144]

Solid Electrolytes: Differing from liquid electrolytes, solid-state electrolytes are also promising for achieving next-generation high-energy sodium batteries, especially sodium metal batteries.[147] Solid-state electrolytes can be composed of inorganic ceramics, organic–polymers or inorganic–polymer composites, which have been discussed above. For more details, NASICONs, thiophosphates and their relatives, and Na β-alumina are the most popular inorganic ceramics with suitable ionic conductivities for solid-state electrolytes (Figure 21b).[104] NASICONs means sodium superionic conductors with the structures of

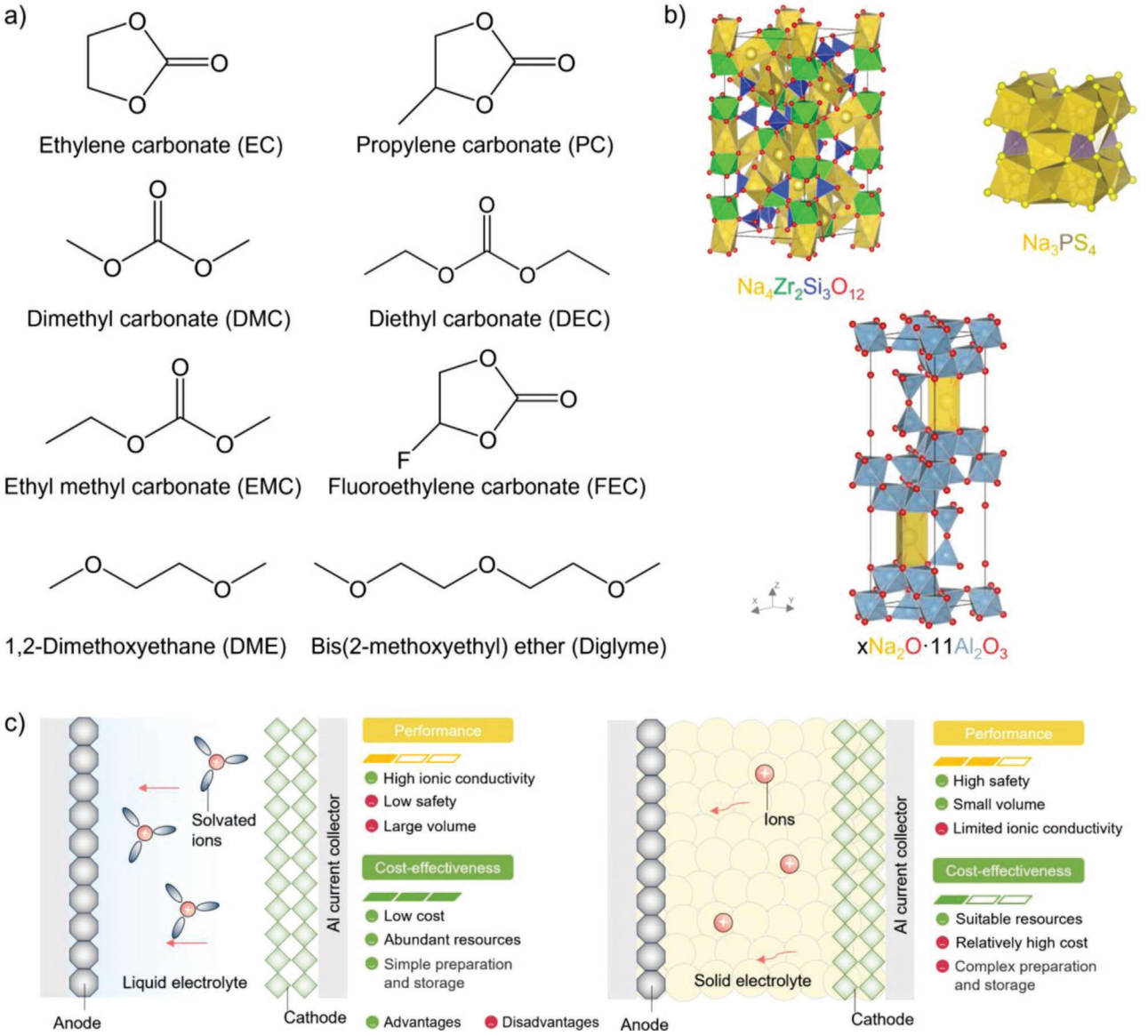

Figure 21. a) Molecular structures of solvents for liquid electrolytes. b) Crystal structures of inorganic ceramics for solid electrolytes. c) Schematic illustrations of the cell configurations with liquid electrolytes or solid electrolytes, combined with the pros and cons of various electrolytes.

$Na_xA_2B_3O_{12}$ (A: Zr, Hf, Sc, etc.; B: Si, P, etc.) such as $Na_4Zr_2Si_3O_{12}$ and $Na_{3.4}Sc_{0.4}Zr_{1.6}Si_2PO_{12}$.[148] Moreover, thiophosphate and their relatives represent a series of compounds such as Na_3PS_4 and $Na_{11}Sn_2PS_{12}$.[149] Although the contained pnictogen elements can enhance the ionic conductivity of traditional oxides and sulfides, the electrochemical stability of solid electrolytes can be reduced at the same time, especially against the sodium metal anode, thus leading to the decomposition of solid electrolytes and the growth of the SEI layer during the reduction process.[11] Therefore, Na β-alumina in the formula of $xNa_2O{\cdot}11Al_2O_3$ can be employed as the trade-off with the balanced ionic conductivity and electrochemical stability.[150]

Compared with inorganic ceramics, organic polymers containing sodium salts can also serve as the solid electrolytes with the advantages of higher flexibility and better interface contact with electrodes, but as mentioned above, the ionic conductivity of polymer-based solid electrolytes is usually lower than that of inorganic ceramics.[151] Poly(ethylene oxide) (PEO) is the most conventional matrix choice of polymer-based solid electrolytes, and many other polymers like polycarbonates, polyamines, polynitriles, and poly(vinylidene fluoride) have also been explored and used.[152–155] To improve the ionic conductivity of polymer-based solid electrolytes, several strategies such as increasing the operation temperature, adding a limited amount of liquid electrolyte to form a quasi-solid-state gel electrolyte or designing inorganic–polymer composite electrolytes have been widely studied.[106,156]

Among all these solid electrolytes, inorganic–polymer composite electrolytes can combine the advantages of inorganic and organic solid electrolytes together and diminish their individual disadvantages, being considered the most promising approach to enable the sodium metal anode by avoiding the creep and suppressing dendrite formation.[157] The rational design and

Table 2. Properties of typical electrolytes for sodium batteries (Reproduced with permission.[6] Copyright 2021, Springer Nature).

Electrolyte	Ionic conductivity at 25 °C [mS cm^{-1}]	Degradation potential [V vs Na^+/Na]
1 M $NaPF_6$ in EC/DMC	7.0	4.5
1 M $NaPF_6$ in diglyme	6.0	4.4
$(Na_2O)_{1.5}(MgO)_{0.05}(Al_2O_3)_{11}$	1	4
$Na_{3.4}Sc_{0.4}Zr_{1.6}Si_2PO_{12}$	4	6
Na_3PS_4	3	2.5
$NaClO_4$ in PC/PEO	1	4.7

large-scale fabrication of solid electrolytes for sodium batteries remain to be investigated for the future industrialization of solid-state sodium-based energy storage devices.

To sum up, liquid electrolytes with excellent ionic conductivity and low cost are an appropriate choice for the current fabrication of sodium batteries. However, the serious safety issues of organic liquid electrolytes or the limited working voltage windows of aqueous electrolytes greatly increase the challenges in the fabrication of high-energy sodium batteries (Figure 21c). Therefore, more effort in developing high-performance and low-cost solid electrolytes can pave the way for high-energy, safe, and sustainable sodium batteries in the future (Figure 21c). Detailed comparison and evaluation of different types of electrolytes based on performance and cost-effectiveness are shown in **Table 2** and Figure 21c.

2.2.4. Electrode Architecture and Cell Assembly

For practical applications, the modification of the electrode architecture and cell assembly should also be considered to ensure the electrochemical performance and minimize the cost of cells in tandem.

For most insertion/intercalation-type electrodes, the limited diffusivity of sodium ions is a more crucial factor than the volume changes for large-scale electrodes. Except for improving the inherent sodium-ion diffusivity of materials, the ideal solution in the battery industry is the modification of particle sizes and morphologies of active materials, thus tuning the phase scales of electrodes where sodium ions diffuse and transfer (Figure 2a).[159] Although the decrease in the length scales can enhance the diffusivity of sodium ions, too small particle sizes of active materials would increase the fabrication costs of electrodes and the requirements of electrode manufacturing techniques.[160] Hence, in future commercial electrodes, more studies on how to optimize the electrode architecture and make a balance between electrochemical performance and cost are needed. Meanwhile, more effort to develop high-performance, low-cost, and sustainable carbon hosts with 3D structures is essential for the architecture of other types of electrodes to solve their problems such as the restricted diffusivity of sodium ions and the uncontrollable volume expansion of active materials (**Figure 22**a).[108,161]

Compared to the commercial lithium-ion batteries based on lithium resources and copper (Cu) foil as the anode current collector, the future sodium-ion battery cell based on the cheaper sodium resource and aluminum (Al) current collectors has the potential to achieve a lower estimated cost.[21] The specific comparison of the two kinds of batteries is listed in Figure 22b, in which we can see the differences in their costs are mainly derived from the cathode and current collector used.[21] Namely, the combination of aluminum and sodium beats the combination of copper and lithium in cost. The current battery industry adopts three cell types which are cylindrical, prismatic, and pouch cells to fitful the different requirements in various practical applications (Figure 22c).[158] The existing production line of lithium-based cells is also applicable to the production of sodium-based cells. For other kinds of sodium batteries including sodium metal batteries, more evaluations of their costs are also favored to assess their possibilities in commercialization and practical applications, but differing from sodium-ion batteries, their most important aim at the current stage is the systematic development of high-performance and low-cost electrode materials and electrolyte systems.

2.3. Sodium Capacitors

According to the visualized statistics of keywords in publications related to sodium capacitors (**Figure 23**), the electrochemical performance still plays a core role. Meanwhile, various carbon materials exhibit their importance in the research on sodium capacitors because of their dominant frequency of appearance and latest average publication year. The studies on sodium capacitors rise in early 2012 and remain in their infancy stage compared to sodium batteries.[10]

As described above, sodium capacitors have a similar configuration to sodium batteries. The main difference between sodium capacitors and sodium batteries is the cathode part. In a sodium capacitor, the cathode stores anions mainly through the physical accumulation of anions on the surface of the cathode, which is a non-Faradic process.[162] Porous carbon materials, therefore, become the essential candidate for the cathode. However, most commercial porous carbon materials are derived from nonrenewable fossil fuel-based resources or belong to expensive carbon nanomaterials such as graphene and carbon nanotubes, which do not fit the sustainable standard of sodium-based energy storage devices.[163] At the same time, the stereotypical pore structures of commercial porous carbon materials usually limit the electrochemical performance of sodium capacitors.[164] Hence, the rational design of porous carbon materials from renewable precursors is needed for producing high-performance and low-cost sodium capacitors. In this section, we focus on analyzing the research progress of carbonaceous materials for sodium capacitors to conclude the design strategies of electrodes and cell assembly principles of sodium capacitors.

2.3.1. Electrodes

The anodes of sodium capacitors are similar to those of sodium batteries because the sodium capacitor actually belongs to a hybrid device with an asymmetric configuration, and its anode should be the battery-type anode that can store sodium ions based on the Faradic process.[10] Therefore, for the detailed discussion on the battery-type anode for sodium-ion storage, please refer to the previous section. Here, we only emphasize

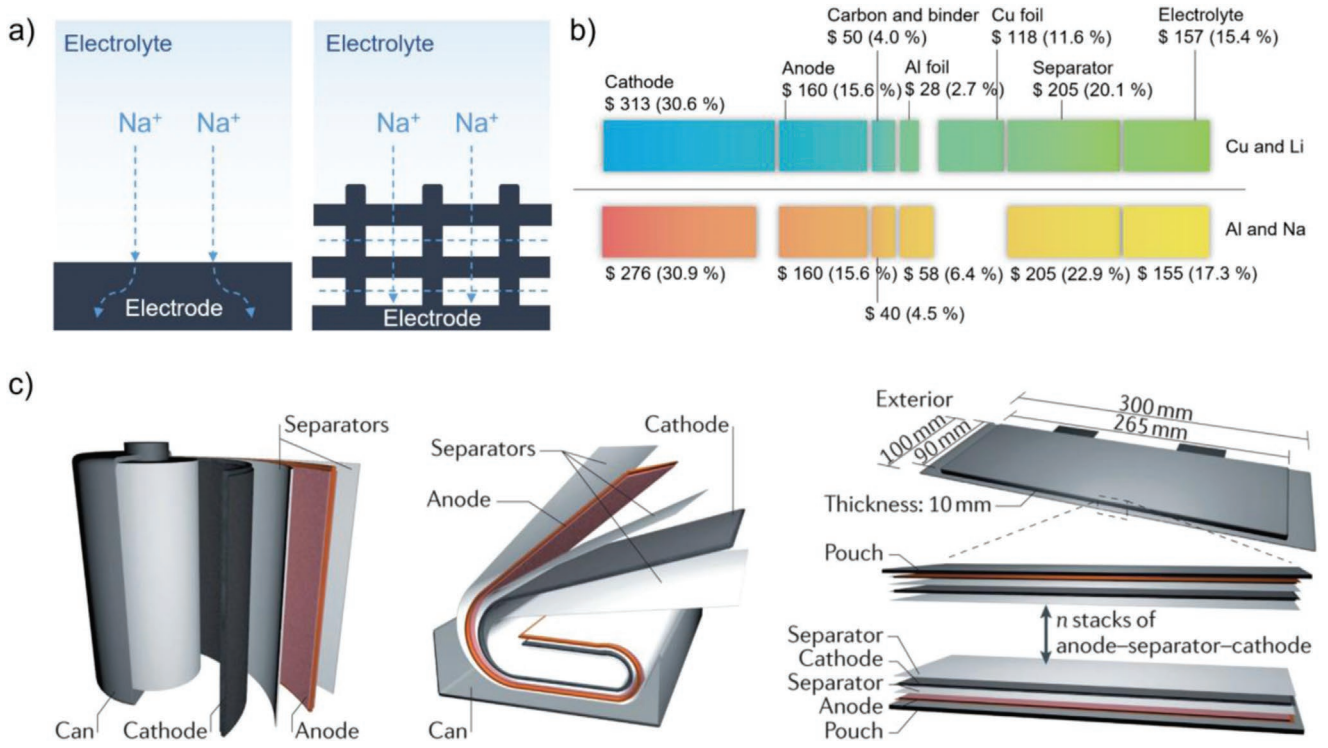

Figure 22. a) The comparison between traditional electrode architectures and novel 3D electrode architectures with optimized structures. b) The cost comparison between the commercial lithium-ion battery cell and the future sodium-ion battery cell (data source collected from ref. [21]). c) Schematic illustrations of cylindrical, prismatic, and pouch cells. Reproduced with permission.[158] Copyright 2016, Springer Nature.

the discussion on the cathode part of sodium capacitors based on a capacitive or pseudocapacitive storage mechanism.

Among various active materials for capacitors including carbonaceous materials, 2D inorganic compounds and conjugated polymers, porous carbon materials are the most popular choice for the cathode of sodium capacitors (**Figure 24**a).[166,167] Porous carbon materials mainly store the anions through the electrochemical double-layer capacitive (EDLC) mechanism (Figure 24b),[168] where the anions are moved to the cathode under the electrical field and adsorbed on the surface of carbon materials to form the first charge layer. Meanwhile, the negative surface charge on the surface can attract the positive charge to form the second charge layer underneath the surface, thus becoming the electrical double layers. With no ions across the interface between the two charge layers, EDLC reactions belong to the non-Faradic process.[168] Sometimes, the functional groups on the surface of carbon materials can interact with anions, which is called pseudocapacitive reactions (Figure 24b).[22] Because the negative ions across the interface between the two charge layers and then combine with positive charges, pseudocapacitive reactions belong to the Faradic process.[22] However, as EDLC and pseudocapacitive reactions occur on the surface or near-surface of carbon materials, they are both surface-controlled reactions with fast kinetics.[169]

Research on sodium capacitors commenced in the 2010s when Kuratani et al.[170] assembled a sodium capacitor by combining sodium predoped hard carbons as the negative electrode and activated carbons as the positive electrode. The working potential window (from 0 to 3.5 V) of the device reported was significantly higher than that of the conventional electrochemical capacitors. Based on the chemical activation or physical activation, activated carbons with porous structures can be achieved. For typically activated carbons, they usually possess a high surface area of around 1000 $m^2\ g^{-1}$ with a high degree of microporosity (<2 nm).[171] Meanwhile, due to the high electronic conductivity and the stable physicochemical properties of typically activated carbons, they are suitable for physically accumulating the active ions on their surface with an excellent stability and reversibility in aqueous electrolytes.[171] However, for sodium capacitors, nonaqueous electrolytes with a higher viscosity and a lower ionic conductivity decrease the electrochemical performance, especially the rate performance, of traditional activated carbons with only micropores. Furthermore, the ionic radius of anions employed in nonaqueous electrolytes such as PF_6^- and ClO_4^- is larger than that of salts in aqueous electrolytes such as OH^- and Cl^-, which further decreases the kinetics of reactions at the cathode part.[172] The high working potential of the cathode part also challenges the stability of traditional activated carbons. Therefore, the development of porous carbons with hierarchical pore structures (i.e., micropores (<2 nm) and mesopores (2–50 nm)), compact particle configurations and ultralong stability is needed for producing high-performance cathodes.[173] Moreover, most traditional activated carbons are derived from nonrenewable fossil fuels, and most high-performance carbon nanomaterials like carbon nanotubes and graphene are expensive.[174] Through "green" activation methods, sustainable porous carbon materials derived from renewable resources can be a promising candidate for the cathode part.[174] For instance, Mitlin and co-workers[165] assembled a

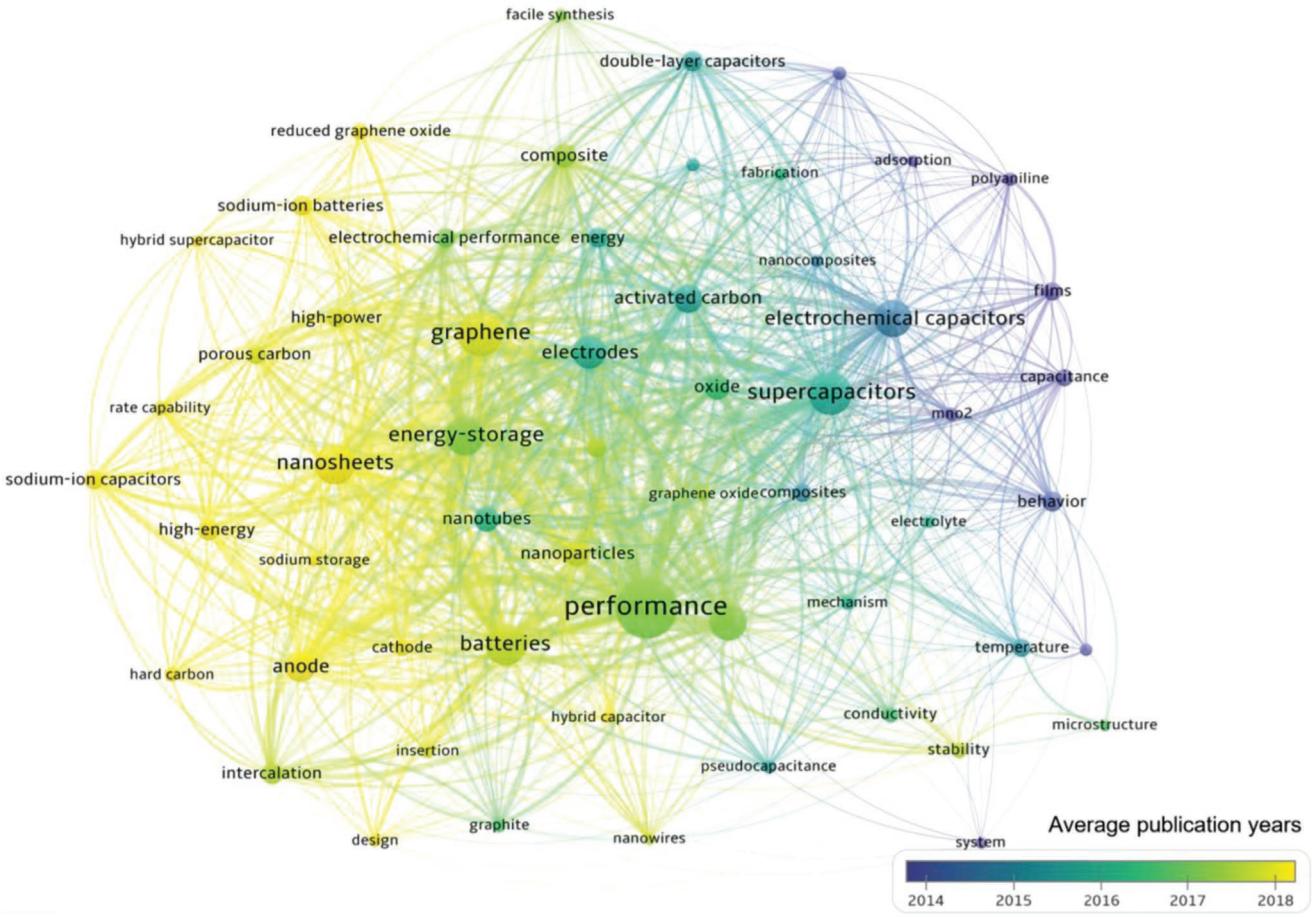

Figure 23. The visualized statistics of keywords in publications related to sodium capacitors since 2001 indexed by Web of Science, where the color represents the average publication year, the size indicates the reported frequency in the literature.

peanut shell prepared hierarchical porous carbons for cathodes and ordered nonporous carbons for anodes (Figure 24c). The outer rough shell was converted into carbon cathodes with a hierarchical pore structure via the KOH-activation method at 800–850 °C in the argon atmosphere, while the inner shell was chosen to be carbonized directly into carbon anodes at 1200 °C. The carbon cathodes were tested in a half cell configuration against metallic sodium and delivered a capacitance of 213 F g^{-1} at 0.1 A g^{-1}, while the carbon anodes exhibit a reversible capacity of 315 mAh g^{-1} at 0.1 A g^{-1}. The acquired sodium-ion capacitors with the all-carbon-based asymmetric configuration showed the integrated high energy and high power densities (201 W h kg^{-1} at 285 W kg^{-1}, 50 W h kg^{-1} at an ultrahigh power density of 16 500 W kg^{-1}), as well as good long-term cycling stability (72% of the capacitance retention after 10 000 cycles at the current density of 6.4 A g^{-1}). Compared to sodium batteries, sodium capacitors with the capacitor-type cathode can possess various advantages such as lower cost and higher power density based on the appropriate sacrifice of energy density (Figure 24d). Although much progress has been achieved in developing nanostructured materials for sodium capacitors, the imbalance of the power capability between anodes and cathodes still inhibits the full energy utilization of anodes, which results from the difference in kinetics that a non-Faradaic adsorption reaction is faster than a Faradaic insertion process (Figure 24d). Consequently, more efforts are required to design anodes with higher power and cathodes with higher energy using suitable materials.

2.3.2. Electrolytes

Sodium capacitors usually employ a similar electrolyte system to sodium batteries, including the liquid electrolytes, gel electrolytes, and solid-state electrolytes. Please refer to the detailed discussion on electrolytes in Section 2.2.

3. Conclusions and Outlook

Due to the limited resource and restricted geographical distribution of lithium, the development of post-lithium technologies is highly necessary at the current stage. Sodium-based energy storage technologies including sodium batteries and sodium capacitors can fulfill the various requirements of different applications such as large-scale energy storage or low-speed/short-distance electrical vehicle.[14] Most knowledge and technical chains of current lithium batteries can be easily transferred to the fabrication of sodium-based energy storage technologies.

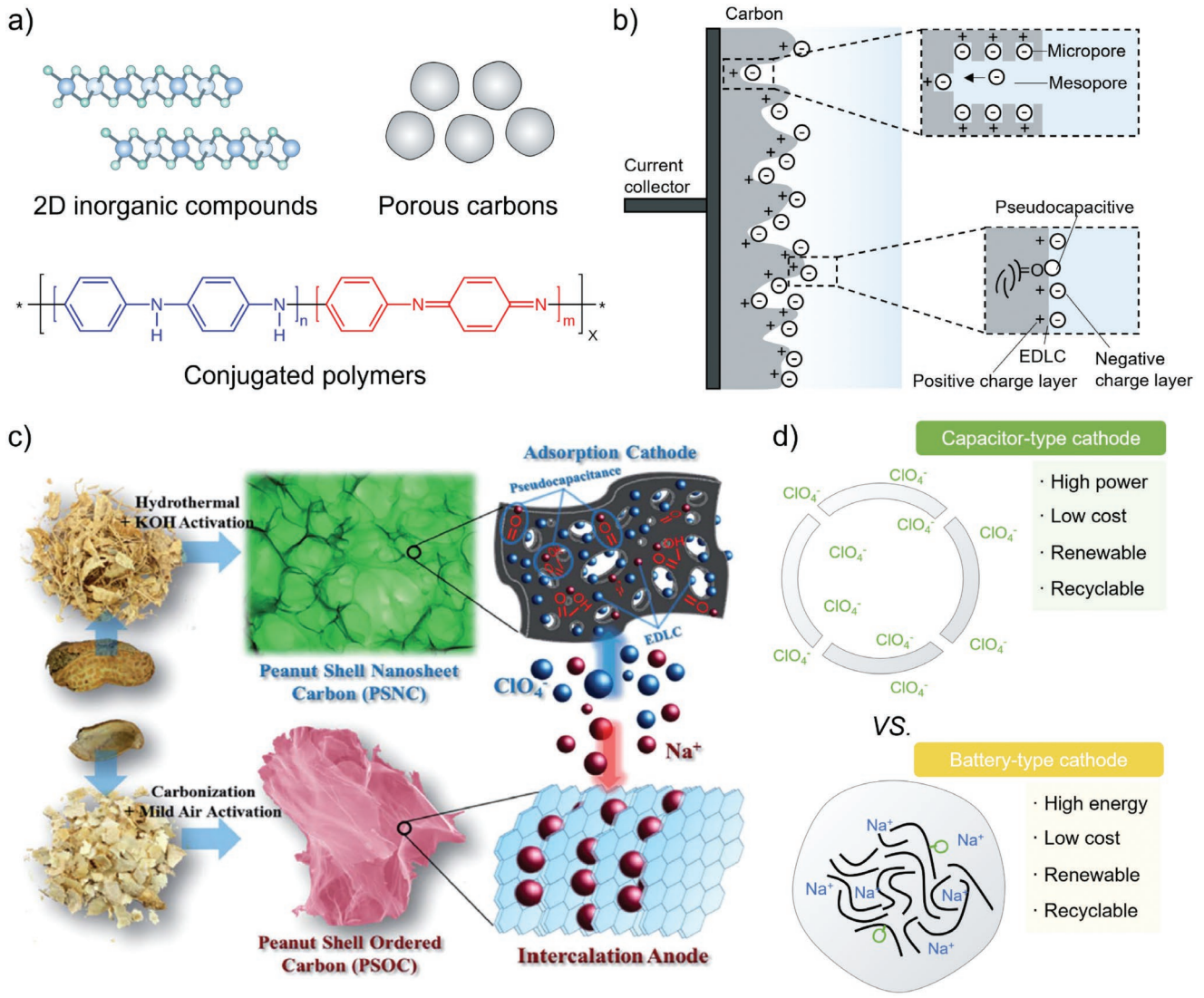

Figure 24. a) Schematic diagrams of active materials for cathodes of sodium capacitors. b) Schematic illustration of porous carbon materials as the cathode to store anions through different mechanisms at various active sites. c) Material synthesis process employed for each electrode in sodium capacitors. Reproduced with permission.[165] Copyright 2015, Royal Society of Chemistry. d) Comparison of the relevant features of cathode and anode in sodium capacitors, combined with their charge storage mechanisms.

Moreover, based on the abundant resource of sodium and the utilization of cheaper aluminum (Al) current collectors, the cost of sodium-based energy storage technologies can be further decreased. Meanwhile, sodium-based energy storage technologies are more appropriate for the applications in extremely cold environments due to their better capacity retention under a low temperature.[18] However, compared to lithium batteries, one of the main challenges of sodium-based energy storage technologies is related to their electrochemical performance, especially the energy density, limited by the natural properties of sodium.

As mentioned in this review, advanced energy materials play a tremendously important role in benefiting the development of sodium-based energy storage technologies by serving as active materials, additives or functional hosts because of their outstanding electrochemical performance. Nevertheless, the fabrication processes of those materials are often linked with rare raw materials, high energy consumption, and toxic chemicals with considerable environmental issues (**Figure 25**a).[51] Hence, to truly achieve not only the performance but also the sustainability of sodium-based energy storage technologies, the renewable resources, and the "greener" fabrication processes including material synthesis and cell assembly are highly required with decreased carbon emissions to simultaneously realize the improved electrochemical performance, the lower cost and the enhanced sustainability of novel sodium-based energy storage technologies (Figure 25a). With the continuous development of sodium-based energy storage technologies, sodium batteries can be employed for off-grid residential or industrial storage, backup power supplies for telecoms, low-speed electric vehicles, and even large-scale energy storage systems, while sodium capacitors can be utilized for off-grid lighting, door locks in automotive subsystems, flashlights, portable hand tools in the future (Figure 25b), thus forming an efficient cooperative energy storage network together with other energy storage technologies. For more information on sodium batteries and capacitors, please refer to these highly related review papers.[2,7–9,18,52,168]

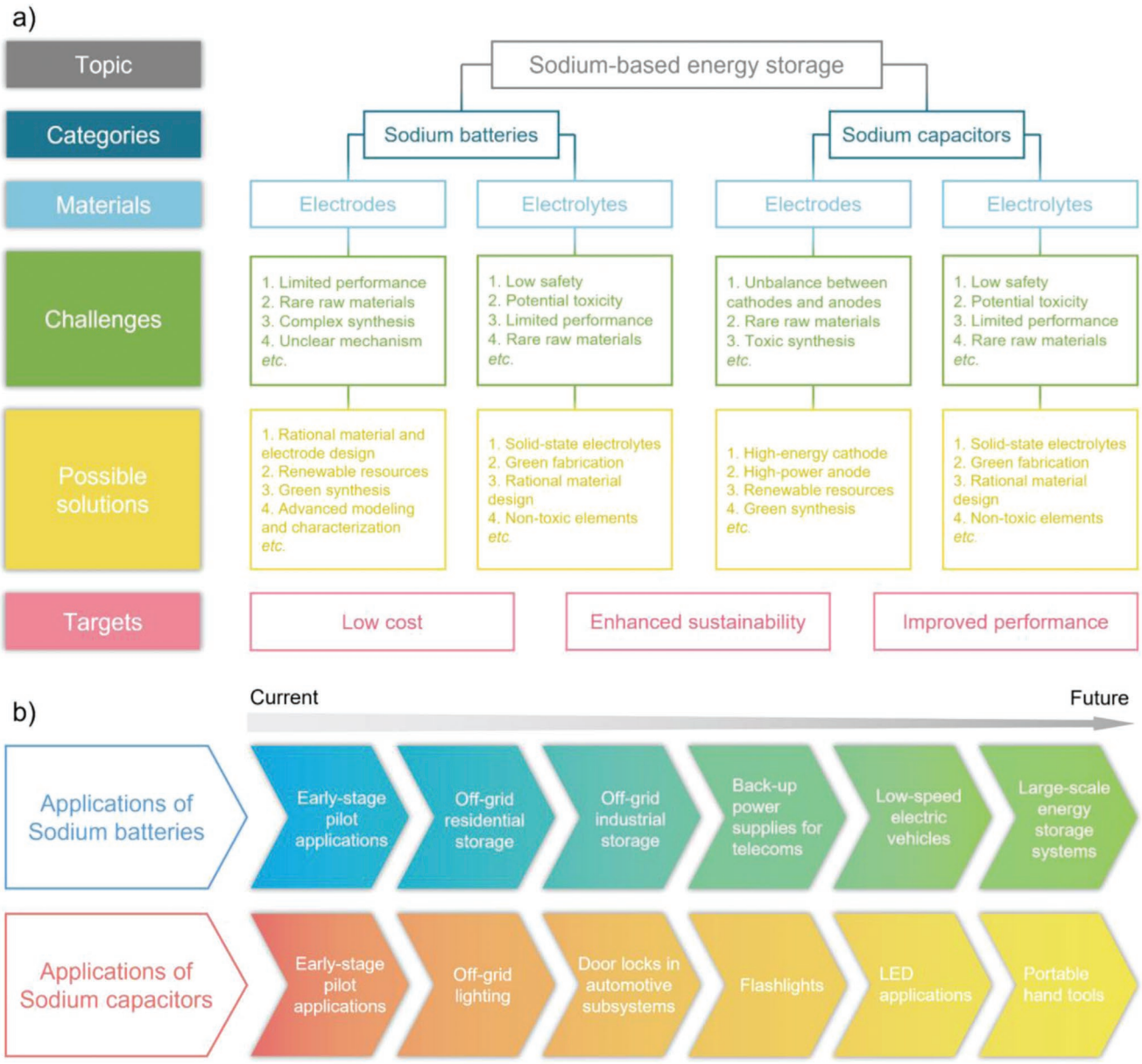

Figure 25. a) Summary of challenges, possible solutions, and targets of sodium-based energy storage technologies. b) The potential applications of sodium batteries and sodium capacitors.

Supporting Information

Supporting Information is available from the Wiley Online Library or from the author.

Acknowledgements

The authors appreciate the grants funded by Science and Technology Facilities Council (STFC) Batteries Network (ST/R006873/1). J.W. acknowledges the China Scholarship Council for the funding support.

Conflict of Interest

The authors declare no conflict of interest.

Keywords

energy storage, performance, sodium, sustainability

Received: May 17, 2022
Revised: May 29, 2022
Published online:

[1] P. V. Kamat, *ACS Energy Lett.* **2019**, *4*, 2757.
[2] M. D. Slater, D. Kim, E. Lee, C. S. Johnson, *Adv. Funct. Mater.* **2013**, *23*, 947.
[3] Y.-G. Lee, S. Fujiki, C. Jung, N. Suzuki, N. Yashiro, R. Omoda, D.-S. Ko, T. Shiratsuchi, T. Sugimoto, S. Ryu, J. H. Ku, T. Watanabe, Y. Park, Y. Aihara, D. Im, I. T. Han, *Nat. Energy* **2020**, *5*, 299.

[4] G. Harper, R. Sommerville, E. Kendrick, L. Driscoll, P. Slater, R. Stolkin, A. Walton, P. Christensen, O. Heidrich, S. Lambert, A. Abbott, K. Ryder, L. Gaines, P. Anderson, *Nature* **2019**, *575*, 75.
[5] B. Dunn, H. Kamath, J. M. Tarascon, *Science* **2011**, *334*, 928.
[6] R. Usiskin, Y. X. Lu, J. Popovic, M. Law, P. Balaya, Y. S. Hu, J. Maier, *Nat. Rev. Mater.* **2021**, *6*, 1020.
[7] N. Yabuuchi, K. Kubota, M. Dahbi, S. Komaba, *Chem. Rev.* **2014**, *114*, 11636.
[8] J. Y. Hwang, S. T. Myung, Y. K. Sun, *Chem. Soc. Rev.* **2017**, *46*, 3529.
[9] J. Ding, W. Hu, E. Paek, D. Mitlin, *Chem. Rev.* **2018**, *118*, 6457.
[10] H. Wang, C. Zhu, D. Chao, Q. Yan, H. J. Fan, *Adv. Mater.* **2017**, 29.
[11] B. Lee, E. Paek, D. Mitlin, S. W. Lee, *Chem. Rev.* **2019**, *119*, 5416.
[12] L. L. Fan, X. F. Li, *Nano Energy* **2018**, *53*, 630.
[13] C. Zhao, Y. Lu, J. Yue, D. Pan, Y. Qi, Y.-S. Hu, L. Chen, *J. Energy Chem.* **2018**, *27*, 1584.
[14] Y. S. Hu, S. Komaba, M. Forsyth, C. Johnson, T. Rojo, *Small Methods* **2019**, *3*, 1900184.
[15] Y. Kato, S. Hori, T. Saito, K. Suzuki, M. Hirayama, A. Mitsui, M. Yonemura, H. Iba, R. Kanno, *Nat. Energy* **2016**, *1*, 16030.
[16] Z. Y. Zhu, Z. Xu, *Renewable Sustainable Energy Rev.* **2020**, *134*, 110308.
[17] M. M. Titirici, R. J. White, N. Brun, V. L. Budarin, D. S. Su, F. del Monte, J. H. Clark, M. J. MacLachlan, *Chem. Soc. Rev.* **2015**, *44*, 250.
[18] E. Goikolea, V. Palomares, S. Wang, I. R. Larramendi, X. Guo, G. Wang, T. Rojo, *Adv. Energy Mater.* **2020**, *10*, 2002055.
[19] H. Liu, X. B. Cheng, J. Q. Huang, S. Kaskel, S. L. Chou, H. S. Park, Q. Zhang, *ACS Mater. Lett.* **2019**, *1*, 217.
[20] D. Castelvecchi, E. Stoye, *Nature* **2019**, *574*, 308.
[21] C. Vaalma, D. Buchholz, M. Weil, S. Passerini, *Nat. Rev. Mater.* **2018**, *3*, 18013.
[22] F. Yu, Z. C. Liu, R. W. Zhou, D. M. Tan, H. X. Wang, F. X. Wang, *Mater. Horiz.* **2018**, *5*, 529.
[23] X. Xiang, K. Zhang, J. Chen, *Adv. Mater.* **2015**, *27*, 5343.
[24] C. X. Zu, H. Li, *Energy Environ. Sci.* **2011**, *4*, 2614.
[25] H. Huang, R. Xu, Y. Feng, S. Zeng, Y. Jiang, H. Wang, W. Luo, Y. Yu, *Adv. Mater.* **2020**, *32*, 1904320.
[26] U. Krewer, F. Röder, E. Harinath, R. D. Braatz, B. Bedürftig, R. Findeisen, *J. Electrochem. Soc.* **2018**, *165*, A3656.
[27] Y. Shao, M. F. El-Kady, J. Sun, Y. Li, Q. Zhang, M. Zhu, H. Wang, B. Dunn, R. B. Kaner, *Chem. Rev.* **2018**, *118*, 9233.
[28] A. R. C. Bredar, A. L. Chown, A. R. Burton, B. H. Farnum, *ACS Appl. Energy Mater.* **2020**, *3*, 66.
[29] F. Xie, Z. Xu, A. C. S. Jensen, F. X. Ding, H. Au, J. Y. Feng, H. Luo, M. Qiao, Z. Y. Guo, Y. X. Lu, A. J. Drew, Y. S. Hu, M. M. Titirici, *J. Mater. Chem. A* **2019**, *7*, 27567.
[30] C. Fang, J. Li, M. Zhang, Y. Zhang, F. Yang, J. Z. Lee, M. H. Lee, J. Alvarado, M. A. Schroeder, Y. Yang, B. Lu, N. Williams, M. Ceja, L. Yang, M. Cai, J. Gu, K. Xu, X. Wang, Y. S. Meng, *Nature* **2019**, *572*, 511.
[31] J. B. Goodenough, Y. Kim, *Chem. Mater.* **2009**, *22*, 587.
[32] S. Komaba, W. Murata, T. Ishikawa, N. Yabuuchi, T. Ozeki, T. Nakayama, A. Ogata, K. Gotoh, K. Fujiwara, *Adv. Funct. Mater.* **2011**, *21*, 3859.
[33] Z. W. Seh, J. Sun, Y. Sun, Y. Cui, *ACS Cent. Sci.* **2015**, *1*, 449.
[34] F. Xie, Z. Xu, A. C. S. Jensen, H. Au, Y. Lu, V. Araullo-Peters, A. J. Drew, Y. S. Hu, M. M. Titirici, *Adv. Funct. Mater.* **2019**, *29*, 1901072.
[35] D. Lin, Y. Liu, Y. Cui, *Nat. Nanotechnol.* **2017**, *12*, 194.
[36] J. W. Xiang, L. Y. Yang, L. X. Yuan, K. Yuan, Y. Zhang, Y. Y. Huang, J. Lin, F. Pan, Y. H. Huang, *Joule* **2019**, *3*, 2334.
[37] J. Peters, D. Buchholz, S. Passerini, M. Weil, *Energy Environ. Sci.* **2016**, *9*, 1744.
[38] Z. Xu, J. Wang, Z. Y. Guo, F. Xie, H. Y. Liu, H. Yadegari, M. Tebyetekerwa, M. P. Ryan, Y. S. Hu, M. M. Titirici, *Adv. Energy Mater.* **2022**, *12*, 2200208.
[39] Y. Q. Fu, Q. L. Wei, G. X. Zhang, S. H. Sun, *Adv. Energy Mater.* **2018**, *8*, 1703058.
[40] F. Xie, Z. Xu, Z. Guo, M.-M. Titirici, *Prog. Energy* **2020**, *2*, 042002.
[41] P. K. Nayak, L. Yang, W. Brehm, P. Adelhelm, *Angew. Chem., Int. Ed.* **2018**, *57*, 102.
[42] K. Kubota, M. Dahbi, T. Hosaka, S. Kumakura, S. Komaba, *Chem. Rec.* **2018**, *18*, 459.
[43] J. B. Goodenough, *Energy Storage Mater.* **2015**, *1*, 158.
[44] Z. Jian, W. Luo, X. Ji, *J. Am. Chem. Soc.* **2015**, *137*, 11566.
[45] J. Zhao, X. X. Zou, Y. J. Zhu, Y. H. Xu, C. S. Wang, *Adv. Funct. Mater.* **2016**, *26*, 8103.
[46] Y. Li, Y. Lu, P. Adelhelm, M. M. Titirici, Y. S. Hu, *Chem. Soc. Rev.* **2019**, *48*, 4655.
[47] H. S. Hou, X. Q. Qiu, W. F. Wei, Y. Zhang, X. B. Ji, *Adv. Energy Mater.* **2017**, *7*, 1602898.
[48] M. Valvo, A. Liivat, H. Eriksson, C. W. Tai, K. Edstrom, *ChemSusChem* **2017**, *10*, 2431.
[49] J. Q. Deng, W. B. Luo, S. L. Chou, H. K. Liu, S. X. Dou, *Adv. Energy Mater.* **2018**, *8*, 1701428.
[50] N. Tapia-Ruiz, A. R. Armstrong, H. Alptekin, M. A. Amores, H. T. Au, J. Barker, R. Boston, W. R. Brant, J. M. Brittain, Y. Chen, M. Chhowalla, Y. S. Choi, S. I. R. Costa, M. C. Ribadeneyra, S. A. Cussen, E. J. Cussen, W. I. F. David, A. V. Desai, S. A. M. Dickson, E. I. Eweka, J. D. Forero-Saboya, C. P. Grey, J. M. Griffin, P. Gross, X. Hua, J. T. S. Irvine, P. Johansson, M. O. Jones, M. Karlsmo, E. Kendrick, et al., *J. Phys.: Energy* **2021**, *3*, 031503.
[51] M. M. Titirici, *Adv. Energy Mater.* **2021**, *11*, 2003700.
[52] W. Luo, F. Shen, C. Bommier, H. Zhu, X. Ji, L. Hu, *Acc. Chem. Res.* **2016**, *49*, 231.
[53] Y. X. Wang, Y. X. Wang, Y. X. Wang, X. M. Feng, W. H. Chen, X. P. Ai, H. X. Yang, Y. L. Cao, *Chem* **2019**, *5*, 2547.
[54] X. W. Dou, I. Hasa, D. Saurel, C. Vaalma, L. M. Wu, D. Buchholz, D. Bresser, S. Komaba, S. Passerini, *Mater. Today* **2019**, *23*, 87.
[55] Q. S. Meng, Y. X. Lu, F. X. Ding, Q. Q. Zhang, L. Q. Chen, Y. S. Hu, *ACS Energy Lett.* **2019**, *4*, 2608.
[56] Y. Y. Huang, Y. H. Zheng, X. Li, F. Adams, W. Luo, Y. H. Huang, L. B. Hu, *ACS Energy Lett.* **2018**, *3*, 1604.
[57] Y. M. Li, Y. S. Hu, M. M. Titirici, L. Q. Chen, X. J. Huang, *Adv. Energy Mater.* **2016**, *6*, 1600659.
[58] K. Tang, L. J. Fu, R. J. White, L. H. Yu, M. M. Titirici, M. Antonietti, J. Maier, *Adv. Energy Mater.* **2012**, *2*, 873.
[59] D. F. Xu, C. J. Chen, J. Xie, B. Zhang, L. Miao, J. Cai, Y. H. Huang, L. N. Zhang, *Adv. Energy Mater.* **2016**, *6*, 1501929.
[60] H. Au, H. Alptekin, A. C. S. Jensen, E. Olsson, C. A. O'Keefe, T. Smith, M. Crespo-Ribadeneyra, T. F. Headen, C. P. Grey, Q. Cai, A. J. Drew, M. M. Titirici, *Energy Environ. Sci.* **2020**, *13*, 3469.
[61] J. M. Stratford, A. K. Kleppe, D. S. Keeble, P. A. Chater, S. S. Meysami, C. J. Wright, J. Barker, M. M. Titirici, P. K. Allan, C. P. Grey, *J. Am. Chem. Soc.* **2021**, *143*, 14274.
[62] Y. Qi, Y. Lu, F. Ding, Q. Zhang, H. Li, X. Huang, L. Chen, Y. S. Hu, *Angew. Chem., Int. Ed.* **2019**, *58*, 4361.
[63] C. L. Zhao, Q. D. Wang, Y. X. Lu, B. H. Li, L. Q. Chen, Y. S. Hu, *Sci. Bull.* **2018**, *63*, 1125.
[64] F. Xie, Z. Xu, Z. Guo, Y. Lu, L. Chen, M.-M. Titirici, Y.-S. Hu, *Sci. China: Chem.* **2021**, *64*, 1679.
[65] Y. S. Wang, W. Zhu, A. G. Fi, C. Kim, K. Zaghib, *Front. Energy Res.* **2019**, *7*, 28.
[66] H. Xiong, M. D. Slater, M. Balasubramanian, C. S. Johnson, T. Rajh, *J. Phys. Chem. Lett.* **2011**, *2*, 2560.
[67] J. Y. Hwang, H. L. Du, B. N. Yun, M. G. Jeong, J. S. Kim, H. Kim, H. G. Jung, Y. K. Sun, *ACS Energy Lett.* **2019**, *4*, 494.
[68] M. N. Tahir, B. Oschmann, D. Buchholz, X. Dou, I. Lieberwirth, M. Panthofer, W. Tremel, R. Zentel, S. Passerini, *Adv. Energy Mater.* **2016**, *6*, 1501489.

[69] A. V. Desai, R. E. Morris, A. R. Armstrong, *ChemSusChem* **2020**, *13*, 4866.
[70] Y. Park, D. S. Shin, S. H. Woo, N. S. Choi, K. H. Shin, S. M. Oh, K. T. Lee, S. Y. Hong, *Adv. Mater.* **2012**, *24*, 3562.
[71] J. Liu, P. Lyu, Y. Zhang, P. Nachtigall, Y. Xu, *Adv. Mater.* **2018**, *30*, 1705401.
[72] F. X. Wu, C. L. Zhao, S. Q. Chen, Y. X. Lu, Y. L. Hou, Y. S. Hu, J. Maier, Y. Yu, *Mater. Today* **2018**, *21*, 960.
[73] J. Sun, H. W. Lee, M. Pasta, H. Yuan, G. Zheng, Y. Sun, Y. Li, Y. Cui, *Nat. Nanotechnol.* **2015**, *10*, 980.
[74] Z. Li, J. Ding, D. Mitlin, *Acc. Chem. Res.* **2015**, *48*, 1657.
[75] L. Baggetto, P. Ganesh, R. P. Meisner, R. R. Unocic, J. C. Jumas, C. A. Bridges, G. M. Veith, *J. Power Sources* **2013**, *234*, 48.
[76] S. Liu, J. K. Feng, X. F. Bian, J. Liu, H. Xu, *Energy Environ. Sci.* **2016**, *9*, 1229.
[77] W. S. Ma, K. B. Yin, H. Gao, J. Z. Niu, Z. Q. Peng, Z. H. Zhang, *Nano Energy* **2018**, *54*, 349.
[78] B. Farbod, K. Cui, W. P. Kalisvaart, M. Kupsta, B. Zahiri, A. Kohandehghan, E. M. Lotfabad, Z. Li, E. J. Luber, D. Mitlin, *ACS Nano* **2014**, *8*, 4415.
[79] L. Y. Hu, X. S. Zhu, Y. C. Du, Y. F. Li, X. S. Zhou, J. C. Bao, *Chem. Mater.* **2015**, *27*, 8138.
[80] H. Y. Lu, L. Wu, L. F. Xiao, X. P. Ai, H. X. Yang, Y. L. Cao, *Electrochim. Acta* **2016**, *190*, 402.
[81] G. L. Chang, Y. F. Zhao, L. Dong, D. P. Wilkinson, L. Zhang, Q. S. Shao, W. Yan, X. L. Sun, J. J. Zhang, *J. Mater. Chem. A* **2020**, *8*, 4996.
[82] J. F. Ni, L. Li, J. Lu, *ACS Energy Lett.* **2018**, *3*, 1137.
[83] Y. Zhu, Y. Wen, X. Fan, T. Gao, F. Han, C. Luo, S. C. Liou, C. Wang, *ACS Nano* **2015**, *9*, 3254.
[84] H. Jin, H. Wang, Z. Qi, D. S. Bin, T. Zhang, Y. Wan, J. Chen, C. Chuang, Y. R. Lu, T. S. Chan, H. Ju, A. M. Cao, W. Yan, X. Wu, H. Ji, L. J. Wan, *Angew. Chem., Int. Ed.* **2020**, *59*, 2318.
[85] M. Hu, Y. Jiang, W. Sun, H. Wang, C. Jin, M. Yan, *ACS Appl. Mater. Interfaces* **2014**, *6*, 19449.
[86] Z.-J. Zhang, Y.-X. Wang, S.-L. Chou, H.-J. Li, H.-K. Liu, J.-Z. Wang, *J. Power Sources* **2015**, *280*, 107.
[87] J. Wang, C. Luo, T. Gao, A. Langrock, A. C. Mignerey, C. Wang, *Small* **2015**, *11*, 473.
[88] T. Hou, X. Sun, D. Xie, M. Wang, A. Fan, Y. Chen, S. Cai, C. Zheng, W. Hu, *Chemistry* **2018**, *24*, 14786.
[89] L. Wang, J. Światowska, S. Dai, M. Cao, Z. Zhong, Y. Shen, M. Wang, *Mater. Today Energy* **2019**, *11*, 46.
[90] J. P. Yang, T. F. Zhou, R. Zhu, X. Q. Chen, Z. P. Guo, J. W. Fan, H. K. Liu, W. X. Zhang, *Adv. Mater. Interfaces* **2016**, *3*, 1500464.
[91] Z. Ali, T. Zhang, M. Asif, L. N. Zhao, Y. Yu, Y. L. Hou, *Mater. Today* **2020**, *35*, 131.
[92] R. A. W. Dryfe, *Curr. Opin. Electrochem.* **2019**, *13*, 119.
[93] D. W. Su, S. X. Dou, G. X. Wang, *Adv. Energy Mater.* **2015**, *5*, 1401205.
[94] C. Zhu, X. Mu, P. A. van Aken, Y. Yu, J. Maier, *Angew. Chem., Int. Ed.* **2014**, *53*, 2152.
[95] H. Zhang, I. Hasa, S. Passerini, *Adv. Energy Mater.* **2018**, *8*, 1702582.
[96] F. Xie, L. Zhang, C. Ye, M. Jaroniec, S. Z. Qiao, *Adv. Mater.* **2019**, *31*, 1800492.
[97] T. Li, A. Qin, L. Yang, J. Chen, Q. Wang, D. Zhang, H. Yang, *ACS Appl. Mater. Interfaces* **2017**, *9*, 19900.
[98] S. Wei, S. Choudhury, J. Xu, P. Nath, Z. Tu, L. A. Archer, *Adv. Mater.* **2017**, *29*, 1605512.
[99] Y. Lee, J. Lee, J. Lee, K. Kim, A. Cha, S. Kang, T. Wi, S. J. Kang, H. W. Lee, N. S. Choi, *ACS Appl. Mater. Interfaces* **2018**, *10*, 15270.
[100] L. M. Suo, O. Borodin, Y. S. Wang, X. H. Rong, W. Sun, X. L. Fan, S. Y. Xu, M. A. Schroeder, A. V. Cresce, F. Wang, C. Y. Yang, Y. S. Hu, K. Xu, C. S. Wang, *Adv. Energy Mater.* **2017**, *7*, 1701189.
[101] L. Jiang, L. Liu, J. Yue, Q. Zhang, A. Zhou, O. Borodin, L. Suo, H. Li, L. Chen, K. Xu, Y. S. Hu, *Adv. Mater.* **2020**, *32*, 1904427.
[102] L. Suo, O. Borodin, T. Gao, M. Olguin, J. Ho, X. Fan, C. Luo, C. Wang, K. Xu, *Science* **2015**, *350*, 938.
[103] Y. Zhao, L. V. Goncharova, A. Lushington, Q. Sun, H. Yadegari, B. Wang, W. Xiao, R. Li, X. Sun, *Adv. Mater.* **2017**, *29*, 1606663.
[104] C. Zhao, L. Liu, X. Qi, Y. Lu, F. Wu, J. Zhao, Y. Yu, Y.-S. Hu, L. Chen, *Adv. Energy Mater.* **2018**, *8*, 1703012.
[105] H. C. Gao, S. Xin, L. G. Xue, J. B. Goodenough, *Chem* **2018**, *4*, 833.
[106] X. L. Cheng, J. Pan, Y. Zhao, M. Liao, H. S. Peng, *Adv. Energy Mater.* **2018**, *8*, 1702184.
[107] Z. Z. Zhang, Q. Q. Zhang, C. Ren, F. Luo, Q. Ma, Y. S. Hu, Z. B. Zhou, H. Li, X. J. Huang, L. Q. Chen, *J. Mater. Chem. A* **2016**, *4*, 15823.
[108] S. S. Chi, X. G. Qi, Y. S. Hu, L. Z. Fan, *Adv. Energy Mater.* **2018**, *8*, 1702764.
[109] B. Sun, P. Li, J. Zhang, D. Wang, P. Munroe, C. Wang, P. H. L. Notten, G. Wang, *Adv. Mater.* **2018**, *30*, 1801334.
[110] B. Sun, P. Xiong, U. Maitra, D. Langsdorf, K. Yan, C. Wang, J. Janek, D. Schroder, G. Wang, *Adv. Mater.* **2020**, *32*, 1903891.
[111] C. W. Wang, H. Xie, L. Zhang, Y. H. Gong, G. Pastel, J. Q. Dai, B. Y. Liu, E. D. Wachsman, L. B. Hu, *Adv. Energy Mater.* **2018**, *8*, 1701963.
[112] W. Yang, W. Yang, L. B. Dong, G. J. Shao, G. X. Wang, X. W. Peng, *Nano Energy* **2021**, *80*, 105563.
[113] L. Ye, M. Liao, T. Zhao, H. Sun, Y. Zhao, X. Sun, B. Wang, H. Peng, *Angew. Chem., Int. Ed.* **2019**, *58*, 17054.
[114] F. Wu, J. H. Zhou, R. Luo, Y. X. Huang, Y. Mei, M. Xie, R. J. Chen, *Energy Storage Mater.* **2019**, *22*, 376.
[115] Z. Xu, Z. Y. Guo, R. Madhu, F. Xie, R. X. Chen, J. Wang, M. Tebyetekerwa, Y. S. Hu, M. M. Titirici, *Energy Environ. Sci.* **2021**, *14*, 6381.
[116] J. X. Wu, J. P. Liu, Z. H. Lu, K. Lin, Y. Q. Lyu, B. H. Li, F. Ciucci, J. K. Kim, *Energy Storage Mater.* **2019**, *23*, 8.
[117] P. Hartmann, C. L. Bender, M. Vracar, A. K. Durr, A. Garsuch, J. Janek, P. Adelhelm, *Nat. Mater.* **2013**, *12*, 228.
[118] J. F. Qian, C. Wu, Y. L. Cao, Z. F. Ma, Y. H. Huang, X. P. Ai, H. X. Yang, *Adv. Energy Mater.* **2018**, *8*, 1702619.
[119] X. Zhang, X. Rui, D. Chen, H. Tan, D. Yang, S. Huang, Y. Yu, *Nanoscale* **2019**, *11*, 2556.
[120] W. J. Li, C. Han, W. L. Wang, F. Gebert, S. L. Chou, H. K. Liu, X. H. Zhang, S. X. Dou, *Adv. Energy Mater.* **2017**, *7*, 1700274.
[121] Z. Dai, U. Mani, H. T. Tan, Q. Yan, *Small Methods* **2017**, *1*, 1700098.
[122] A. Tripathi, A. Rudola, S. R. Gajjela, S. B. Xi, P. Balaya, *J. Mater. Chem. A* **2019**, *7*, 25944.
[123] N. Yabuuchi, M. Kajiyama, J. Iwatate, H. Nishikawa, S. Hitomi, R. Okuyama, R. Usui, Y. Yamada, S. Komaba, *Nat. Mater.* **2012**, *11*, 512.
[124] X. Rong, E. Hu, Y. Lu, F. Meng, C. Zhao, X. Wang, Q. Zhang, X. Yu, L. Gu, Y.-S. Hu, H. Li, X. Huang, X.-Q. Yang, C. Delmas, L. Chen, *Joule* **2019**, *3*, 503.
[125] X. H. Rong, J. Liu, E. Y. Hu, Y. J. Liu, Y. Wang, J. P. Wu, X. Q. Yu, K. Page, Y. S. Hu, W. L. Yang, H. Li, X. Q. Yang, L. Q. Chen, X. J. Huang, *Joule* **2018**, *2*, 125.
[126] R. A. House, J.-J. Marie, M. A. Pérez-Osorio, G. J. Rees, E. Boivin, P. G. Bruce, *Nat. Energy* **2021**, *6*, 781.
[127] R. A. House, U. Maitra, M. A. Perez-Osorio, J. G. Lozano, L. Jin, J. W. Somerville, L. C. Duda, A. Nag, A. Walters, K. J. Zhou, M. R. Roberts, P. G. Bruce, *Nature* **2020**, *577*, 502.
[128] T. Jin, H. Li, K. Zhu, P. F. Wang, P. Liu, L. Jiao, *Chem. Soc. Rev.* **2020**, *49*, 2342.
[129] Y. Qi, Z. Tong, J. Zhao, L. Ma, T. Wu, H. Liu, C. Yang, J. Lu, Y.-S. Hu, *Joule* **2018**, *2*, 2348.
[130] Y. Jiang, Z. Z. Yang, W. H. Li, L. C. Zeng, F. S. Pan, M. Wang, X. Wei, G. T. Hu, L. Gu, Y. Yu, *Adv. Energy Mater.* **2015**, *5*, 1402104.
[131] M. Law, V. Ramar, P. Balaya, *J. Power Sources* **2017**, *359*, 277.

[132] K. Hurlbutt, S. Wheeler, I. Capone, M. Pasta, *Joule* **2018**, *2*, 1950.
[133] Y. You, X. L. Wu, Y. X. Yin, Y. G. Guo, *Energy Environ. Sci.* **2014**, *7*, 1643.
[134] J. Song, L. Wang, Y. Lu, J. Liu, B. Guo, P. Xiao, J. J. Lee, X. Q. Yang, G. Henkelman, J. B. Goodenough, *J. Am. Chem. Soc.* **2015**, *137*, 2658.
[135] L. W. Jiang, Y. X. Lu, C. L. Zhao, L. L. Liu, J. N. Zhang, Q. Q. Zhang, X. Shen, J. M. Zhao, X. Q. Yu, H. Li, X. J. Huang, L. Q. Chen, Y. S. Hu, *Nat. Energy* **2019**, *4*, 495.
[136] P. Adelhelm, P. Hartmann, C. L. Bender, M. Busche, C. Eufinger, J. Janek, *Beilstein J. Nanotechnol.* **2015**, *6*, 1016.
[137] X. Xu, D. Zhou, X. Qin, K. Lin, F. Kang, B. Li, D. Shanmukaraj, T. Rojo, M. Armand, G. Wang, *Nat. Commun.* **2018**, *9*, 3870.
[138] M. Salama, Rosy, R. Attias, R. Yemini, Y. Gofer, D. Aurbach, M. Noked, *ACS Energy Lett.* **2019**, *4*, 436.
[139] N. Ortiz-Vitoriano, T. P. Batcho, D. G. Kwabi, B. Han, N. Pour, K. P. Yao, C. V. Thompson, Y. Shao-Horn, *J. Phys. Chem. Lett.* **2015**, *6*, 2636.
[140] H. Yuan, T. Liu, Y. Liu, J. Nai, Y. Wang, W. Zhang, X. Tao, *Chem. Sci.* **2019**, *10*, 7484.
[141] M. M. Ottakam Thotiyl, S. A. Freunberger, Z. Peng, P. G. Bruce, *J. Am. Chem. Soc.* **2013**, *135*, 494.
[142] A. Ponrouch, E. Marchante, M. Courty, J. M. Tarascon, M. R. Palacin, *Energy Environ. Sci.* **2012**, *5*, 8572.
[143] Y. Q. Li, Y. Yang, Y. X. Lu, Q. Zhou, X. G. Qi, Q. S. Meng, X. H. Rong, L. Q. Chen, Y. S. Hu, *ACS Energy Lett.* **2020**, *5*, 1156.
[144] Y. Yamada, J. Wang, S. Ko, E. Watanabe, A. Yamada, *Nat. Energy* **2019**, *4*, 269.
[145] Y. Li, Y. Li, A. Pei, K. Yan, Y. Sun, C. L. Wu, L. M. Joubert, R. Chin, A. L. Koh, Y. Yu, J. Perrino, B. Butz, S. Chu, Y. Cui, *Science* **2017**, *358*, 506.
[146] K. Westman, R. Dugas, P. Jankowski, W. Wieczorek, G. Gachot, M. Morcrette, E. Irisarri, A. Ponrouch, M. R. Palacin, J. M. Tarascon, P. Johansson, *ACS Appl. Energy Mater.* **2018**, *1*, 2671.
[147] L. Fan, S. Y. Wei, S. Y. Li, Q. Li, Y. Y. Lu, *Adv. Energy Mater.* **2018**, *8*, 1702657.
[148] Z. Z. Zhang, Z. Y. Zou, K. Kaup, R. J. Xiao, S. Q. Shi, M. Avdeev, Y. S. Hu, D. Wang, B. He, H. Li, X. J. Huang, L. F. Nazar, L. Q. Chen, *Adv. Energy Mater.* **2019**, *9*, 1902373.
[149] T. Famprikis, O. U. Kudu, J. A. Dawson, P. Canepa, F. Fauth, E. Suard, M. Zbiri, D. Dambournet, O. J. Borkiewicz, H. Bouyanfif, S. P. Emge, S. Cretu, J. N. Chotard, C. P. Grey, W. G. Zeier, M. S. Islam, C. Masquelier, *J. Am. Chem. Soc.* **2020**, *142*, 18422.
[150] M. C. Bay, M. Wang, R. Grissa, M. V. F. Heinz, J. Sakamoto, C. Battaglia, *Adv. Energy Mater.* **2019**, *10*, 1902899.
[151] Y. W. Zheng, Q. W. Pan, M. Clites, B. W. Byles, E. Pomerantseva, C. Y. Li, *Adv. Energy Mater.* **2018**, *8*, 1801885.
[152] A. Boschin, P. Johansson, *Electrochim. Acta* **2015**, *175*, 124.
[153] M. Y. Zhang, M. X. Li, Z. Chang, Y. F. Wang, J. Gao, Y. S. Zhu, Y. P. Wu, W. Huang, *Electrochim. Acta* **2017**, *245*, 752.
[154] K. K. Kumar, M. Ravi, Y. Pavani, S. Bhavani, A. K. Sharma, V. V. R. N. Rao, *J. Membr. Sci.* **2014**, *454*, 200.
[155] Y. L. Ni'mah, M.-Y. Cheng, J. H. Cheng, J. Rick, B.-J. Hwang, *J. Power Sources* **2015**, *278*, 375.
[156] X. W. Yu, A. Manthiram, *Matter* **2019**, *1*, 439.
[157] Y. Gao, Z. Yan, J. L. Gray, X. He, D. Wang, T. Chen, Q. Huang, Y. C. Li, H. Wang, S. H. Kim, T. E. Mallouk, D. Wang, *Nat. Mater.* **2019**, *18*, 384.
[158] J. W. Choi, D. Aurbach, *Nat. Rev. Mater.* **2016**, *1*, 16013.
[159] P. Lu, Y. Sun, H. F. Xiang, X. Liang, Y. Yu, *Adv. Energy Mater.* **2018**, *8*, 1702434.
[160] H. Hou, C. E. Banks, M. Jing, Y. Zhang, X. Ji, *Adv. Mater.* **2015**, *27*, 7861.
[161] A. B. Jorge, R. Jervis, A. P. Periasamy, M. Qiao, J. Y. Feng, L. N. Tran, M. M. Titirici, *Adv. Energy Mater.* **2020**, *10*, 1902494.
[162] Z. Xu, F. Xie, J. Wang, H. Au, M. Tebyetekerwa, Z. Guo, S. Yang, Y. S. Hu, M. M. Titirici, *Adv. Funct. Mater.* **2019**, *29*, 1903895.
[163] F. Wang, X. Wang, Z. Chang, X. Wu, X. Liu, L. Fu, Y. Zhu, Y. Wu, W. Huang, *Adv. Mater.* **2015**, *27*, 6962.
[164] Y. E. Zhu, L. P. Yang, J. Sheng, Y. N. Chen, H. C. Gu, J. P. Wei, Z. Zhou, *Adv. Energy Mater.* **2017**, *7*.
[165] J. Ding, H. L. Wang, Z. Li, K. Cui, D. Karpuzov, X. H. Tan, A. Kohandehghan, D. Mitlin, *Energy Environ. Sci.* **2015**, *8*, 941.
[166] N. Kurra, M. Alhabeb, K. Maleski, C. H. Wang, H. N. Alshareef, Y. Gogotsi, *ACS Energy Lett.* **2018**, *3*, 2094.
[167] W. Zuo, R. Li, C. Zhou, Y. Li, J. Xia, J. Liu, *Adv. Sci.* **2017**, *4*, 1600539.
[168] V. Aravindan, M. Ulaganathan, S. Madhavi, *J. Mater. Chem. A* **2016**, *4*, 7538.
[169] X. Wang, S. Kajiyama, H. Iinuma, E. Hosono, S. Oro, I. Moriguchi, M. Okubo, A. Yamada, *Nat. Commun.* **2015**, *6*, 6544.
[170] K. Kuratani, M. Yao, H. Senoh, N. Takeichi, T. Sakai, T. Kiyobayashi, *Electrochim. Acta* **2012**, *76*, 320.
[171] L. Zhao, L. Z. Fan, M. Q. Zhou, H. Guan, S. Qiao, M. Antonietti, M. M. Titirici, *Adv. Mater.* **2010**, *22*, 5202.
[172] L. Fan, K. Lin, J. Wang, R. Ma, B. Lu, *Adv. Mater.* **2018**, *30*, 1800804.
[173] M. Sevilla, A. B. Fuertes, *ChemSusChem* **2016**, *9*, 1880.
[174] M. Sevilla, G. A. Ferrero, A. B. Fuertes, *Chem. Mater.* **2017**, *29*, 6900.

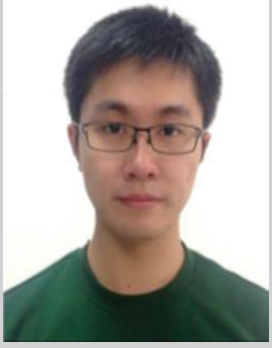

Zhen Xu received his B.Eng. in Polymer Materials and Engineering from Donghua University in 2017. After that, He did his Ph.D. in Chemical Engineering at Imperial College London. Now he is a research fellow at Yusuf Hamied Department of Chemistry, University of Cambridge. His research interests include sustainable carbon materials for electrochemical energy storage and CO_2 capture.

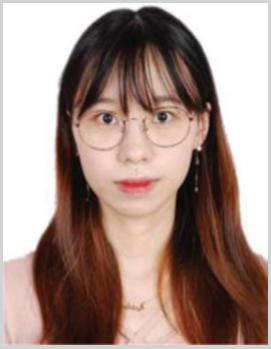

Jing Wang received her B.Eng. degree (2017) in Composites Materials and Engineering at Donghua University and M.Sc. degree (2018) in Advanced Composites at University of Bristol. She is currently a Ph.D. researcher at the Bristol Composites Institute, University of Bristol. Her current research interests focus on the development of sustainable, cellulose-derived nanocomposites for next-generation energy storage technologies, including sodium/potassium-ion batteries and sodium-metal batteries.